

1 Amplification is the Primary Mode of Gene-by-Sex Interaction 2 in Complex Human Traits

3 Carrie Zhu^{1,2}, Matthew J. Ming^{1,2}, Jared M. Cole^{1,2}, Michael D. Edge³, Mark Kirkpatrick², Arbel Harpak^{1,2,*}

4 ¹ Department of Population Health, The University of Texas at Austin, Austin, TX

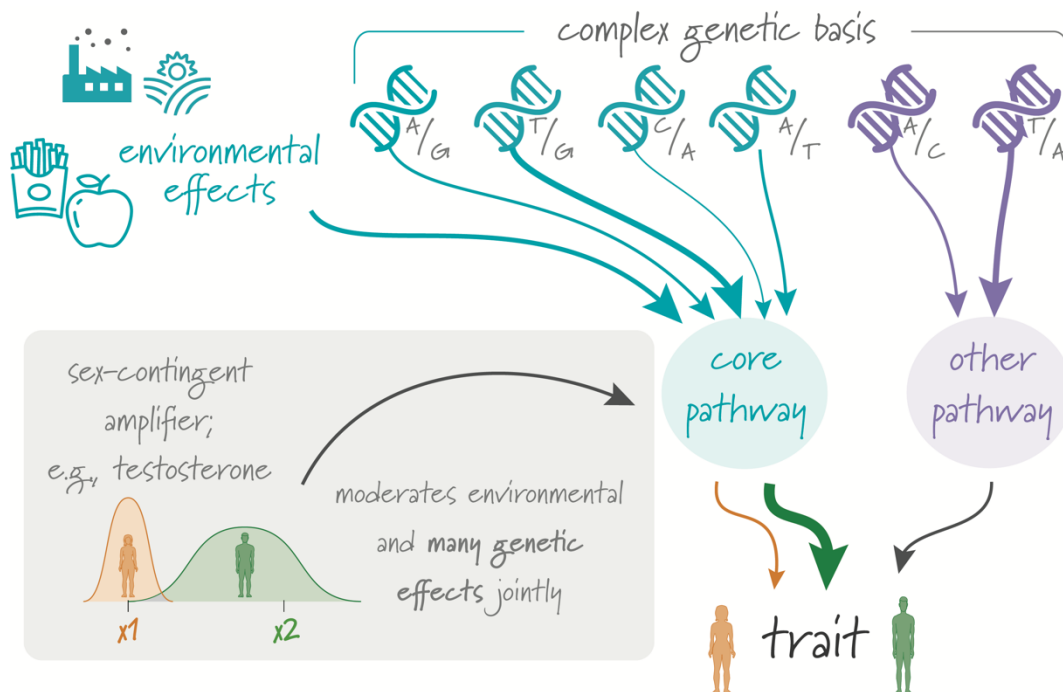
5 ² Department of Integrative Biology, The University of Texas at Austin, Austin, TX

6 ³ Department of Quantitative and Computational Biology, University of Southern California, Los Angeles, CA

7 * To whom correspondence should be addressed: arbelharpak@utexas.edu

8 Abstract

9 Sexual dimorphism in complex traits is suspected to be in part due to widespread gene-by-sex
10 interactions (GxSex), but empirical evidence has been elusive. Here, we infer the mixture of ways
11 polygenic effects on physiological traits covary between males and females. We find that GxSex
12 is pervasive but acts primarily through systematic sex differences in the magnitude of many
13 genetic effects (“amplification”), rather than in the identity of causal variants. Amplification patterns
14 account for sex differences in trait variance. In some cases, testosterone may mediate
15 amplification. Finally, we develop a population-genetic test linking GxSex to contemporary natural
16 selection and find evidence for sexually antagonistic selection on variants affecting testosterone
17 levels. Taken together, our results suggest that the amplification of polygenic effects is a common
18 mode of GxSex that may contribute to sex differences and fuel their evolution.
19



20

21 Introduction

22 Genetic effects can depend on context. If the distribution of contexts differs between groups of
23 people, as they do for males and females, so should the average genetic effects on traits^{1,2}. In
24 particular, such gene-by-sex interaction (GxSex) may be a result of sex differences in bodily,
25 environmental and social contexts or epistatic interaction with sex chromosomes. Sex differences
26 in genetic effects on complex traits are clearly of high evolutionary³⁻⁸ and translational⁹⁻¹⁷
27 importance. Yet with the exception of testosterone levels¹⁸⁻²¹, the basis of sexual dimorphism in
28 complex traits is not well understood¹³. To date, empirical evidence for GxSex in GWAS data—
29 whether focused on identifying large GxSex effects at individual loci or by estimating genetic
30 correlations between the sexes for polygenic traits—has been lacking.

31 Here, we set out to study governing principles of GxSex in complex human traits and
32 explain why current approaches for characterizing GxSex may be lacking for this goal. We then
33 suggest a mode of GxSex that may have gone largely underappreciated: A systematic difference
34 in the magnitude of effect of many variants between the sexes, which we refer to as
35 “amplification”²². Amplification can happen for a large set of variants regulating a specific pathway
36 if the pathway responds to a shared cue²³⁻²⁶. In classic hypothesis-testing approaches that test
37 for a GxSex effect separately in each variant, the signal of amplification may be crushed under
38 the multiple hypothesis burden. On the other hand, even state-of-the-art tools designed with
39 complex traits in mind may miss amplification signals: They often treat genetic correlation
40 (between GWAS estimates based on samples from two environments) as a litmus test for whether
41 effects are the same in two groups²⁷⁻³¹, but correlations are scaleless and thus may entirely miss
42 amplification effects.

43 We developed a new approach for flexibly characterizing a mixture of male-female genetic
44 covariance relationships and applied it to 27 physiological traits in the UK Biobank. We found that
45 amplification is pervasive across traits, and that considering amplification helps explain sex
46 differences in phenotypic variance. Finally, we consider an implication of polygenic GxSex for
47 sexually antagonistic selection: Our model confirms that variants that affect traits may be subject
48 to sexually antagonistic selection when male and female trait optima are very different or,
49 surprisingly, even if the trait optima are very similar. We developed a novel test for sexually
50 antagonistic polygenic selection, which connects GxSex to signals of contemporary viability

51 selection. Using this test, we find subtle evidence of sexually antagonistic selection on variants
52 affecting testosterone levels.

53

54 **Results**

55 **The limited scope of single-locus analysis.** We conducted GWASs stratified by sex
56 chromosome karyotype for 27 continuous physiological traits in the UKB using a sample of ~150K
57 individuals with two X chromosomes and another sample of ~150K individuals with XY, and a
58 combined sample that included both the XX and XY samples. We chose to analyze traits with
59 SNP heritabilities over 7.5% in the combined sample, to have higher statistical power. While there
60 is not a strict one-to-one relationship between sex chromosome karyotype and biological sex, we
61 label XX individuals as females and XY individuals as males, and view these labels as capturing
62 group differences in distributions of contexts for autosomal effects, rather than as a
63 dichotomy^{14,17,32}. Throughout, we analyze GWAS on the raw measurement units as provided by
64 UKB. (See note on the rationale behind this choice in the section **Amplification of genetic
65 effects is the primary mode of GxSex**).

66 Among the 27 traits, we observed substantial discordance between males and females in
67 associations with the trait only for testosterone and waist:hip ratio (whether or not it is adjusted
68 for BMI; **Fig. S1**). For testosterone, as noted in previous analyses, associated genes are often in
69 separate pathways in males and females^{18,20}. This is reflected in the small overlap of genes
70 neighboring top associations in our GWAS. For example, in females, the gene CYP3A7 is
71 involved in the hydroxylation of testosterone, resulting in its inactivation. In males, FKBP4 plays
72 a role in the downstream signaling of testosterone on the hypothalamus. Both genes, to our
73 knowledge, do not affect testosterone levels in the other sex.

74 For waist:hip ratio, we saw multiple associations in females only, such as variants near
75 ADAMTS9, a gene involved in insulin sensitivity³³. As previous work established^{18,20,21},
76 testosterone and waist:hip ratio are the exception, not the rule: Most traits did not display many
77 sex differences in top associations. For instance, arm fat-free mass, a highly heritable dimorphic
78 trait, showed near-perfect concordance in significant loci (**Fig. S1**). A previous study²¹ examining
79 the concordance in top associations between males and females found few uniquely-associated
80 SNPs (<20) across the 84 continuous traits they studied; waist:hip ratio was an exception with

81 100 associations unique to one sex. Considering the evidence for the polygenicity of additive
82 genetic variation affecting many complex traits^{34–36}, it stands to reason that looking beyond lead
83 associations, through a polygenic prism, may aid in the characterization of non-additive effects
84 (such as GxSex) as well.

85

86 **The limited scope of analyzing GxSex via heritability differences and genetic correlations.**

87 We therefore turned to consider the polygenic nature of GxSex, first by employing commonly-
88 used approaches: comparing sex-specific SNP heritabilities and examining genetic correlations.
89 We used LD Score Regression (LDSC)^{31,37} to estimate these for each trait. In most traits (17/27),
90 males and females had a genetic correlation greater than 0.9. Testosterone had the lowest
91 genetic correlation of 0.01, which suggests very little sharing of signals between males and
92 females (see similar results by Flynn et al.²⁰ and Sinnott-Armstrong et al.¹⁸).

93 For the majority of traits (18/27), male and female heritabilities were both greater than the
94 heritability in a sample that included both sexes. For instance, in arm fat-free mass (right), the
95 heritability in the both-sex sample was 0.232 (± 0.009), while the heritabilities for male and female
96 were 0.279 (± 0.012) and 0.255 (± 0.011), respectively. In particular, all body mass-related traits,
97 excluding BMI-adjusted waist:hip ratio, had greater sex-specific heritabilities (**Fig. 1**).

98 In addition, we noticed a trend in which, as the genetic correlation decreased, the
99 difference between the heritabilities within each sex and in the sample combining both sexes
100 tended to become larger (Pearson $r = -0.88$, paired t-test p-value = 10^{-10} , **Fig. 1**). Nonetheless,
101 several traits with genetic correlation above 0.9 also present relatively large sex differences in
102 heritability: For example, diastolic blood pressure and arm fat-free mass (left) had differences of
103 5.2% (two-sample t-test p-value = $3 \cdot 10^{-6}$) and 3.4% (two-sample t-test p-value = 0.04),
104 respectively. These examples are incompatible with a model of pervasive uncorrelated genetic
105 effects driving sex-specific genetic contributions to variation in the trait (**Table 1**, second model).

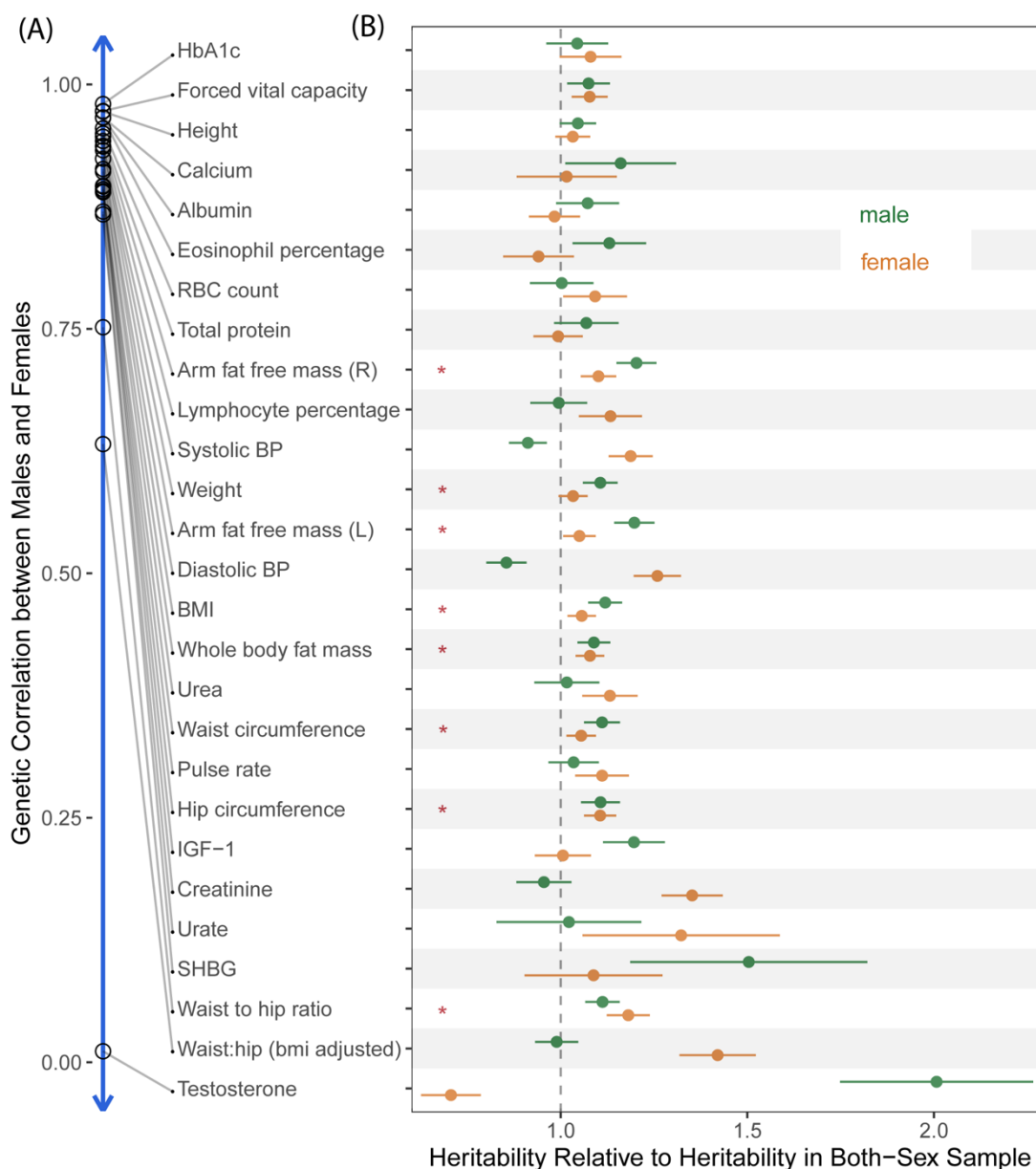
106 We therefore considered two other alternative hypotheses under a simple additive model
107 of variance in a trait. Differences in heritability are either due to sex differences in genetic variance,
108 in environmental variance, or both. If genetic effects are similar, differences in environmental
109 variance alone could cause heritability differences (**Table 1**, first model). But as we show in the
110 **Methods** section, under such a model, the heritability in the combined sample cannot be smaller
111 than both sex-specific heritabilities.

112 Therefore, the observation of higher sex-specific heritabilities for most traits suggests that
113 the genetic variance must differ between males and females. Given the random segregation of
114 autosomal alleles, independent of an individual's sex chromosome karyotype, and assuming,
115 further, that there is little-to-no interaction of sex and genotype affecting participation in the UKB³⁸,
116 UKB allele frequencies in males and females are expected to be very similar. Thus, this
117 observation suggests that causal genetic effects differ between males and females for most traits
118 analyzed.





119 A last hypothesis that might tie together the observations in **Table 1** is a less appreciated
120 mode of GxSex, amplification. Namely, that the identity and direction of effects are largely shared
121 between sexes (leading to high genetic correlation), but the magnitude of genetic effects differs—
122 e.g., larger genetic effects on blood pressure in females—which in turn lead to differences in
123 genetic variance (**Table 1**, third model).

124 We can test the hypothesis that amplification acts systematically—across a large fraction
125 of causal variants—by examining the effects of polygenic scores (PGSs), genetic predictors of a
126 complex trait. Under this hypothesis, regardless of whether the PGS is estimated in a sample of
127 males, females, or a combined sample of both males and females, it should be predictive in both
128 sexes, since the causal variants and the direction of their effects are shared and the magnitude
129 is correlated (**Table 1**, third model). At the same time, in the sex for which genetic effects are
130 larger, the effect of the PGS is expected to be larger. To evaluate evidence for the systematic
131 amplification model, we estimated PGSs based on our sex-specific GWASs, and examined their
132 effect in both sexes. For some traits, like albumin and lymphocyte percentage, the effects of the
133 same PGS on trait value in males and females were statistically indistinguishable (**Fig. 2A,E,I,J**).
134 In a few other traits, such as diastolic blood pressure, the result was contingent on the sample in
135 which the PGS was estimated (**Fig. 2C,G,I,J**). However, for roughly half of the traits examined,
136 regardless of the sample in which the PGS was derived, the effect of the PGS was predictive in
137 both sexes yet significantly larger in one of the sexes (17/27 traits with t-test p-value < 0.05 using
138 the PGS derived from the males sample; 13/27 using the PGS derived from the females sample;
139 **Fig. 2B,D,F,H,I,J**). These observations are consistent with systematic amplification.

140 The results presented in **Figs. 1,2** suggested to us that various modes of polygenic GxSex
141 ought to be jointly evaluated. None of the hypothesized rules of thumb (**Table 1**) for interpreting
142 genetic correlations and sex differences in heritability worked across all traits (see also relevant



143
 144 **Figure 1: Heritabilities and Genetic Correlations Cannot Fully Distinguish Models of GxSex.** (A) Genetic
 145 correlations between the male and females, estimated using bi-variate LD Score Regression, are shown in descending
 146 order. (B) The x-axis represents the relative heritability, i.e., the SNP heritability divided by the SNP heritability
 147 estimated in the sample with both sexes combined. Red asterisks show body-mass related traits with greater
 148 heritabilities in both sex-specific samples than in the sample combining both sexes.

Model	Motivation	Illustration of Effect Covariance	Expectation from Heritability Analysis
No GxSex	Little previous evidence for GxSex		(a) h_m^2 can only differ from h_f^2 through environmental variance differences (b) $h_m^2 < h^2$ or $h_f^2 < h^2$
Weakly or negatively correlated genetic effects	Sexual dimorphism is pervasive and heritable contribution is expected to lie primarily in autosomes		(a) Low or negative genetic correlation (b) $h_m^2, h_f^2 > h^2$, and the larger the difference, the lower the genetic correlation
Highly correlated effects, difference in magnitude ("amplification")	Response to cues such as testosterone; evidence for GxE in non-human organisms		(a) High genetic correlation (b) h_m^2 or $h_f^2 < h^2$
Mixture of covariance relationships	Heritability analysis often incompatible with either model or cannot distinguish between models		Compatible with all observations; motivates: (a) Direct estimation of genetic effect covariance, rather than sole reliance on heritability estimates (b) Modeling mixture components

149

150

151

152

153

154

155

156

157

158

159

160

161

162

163

164

165

166

167

168

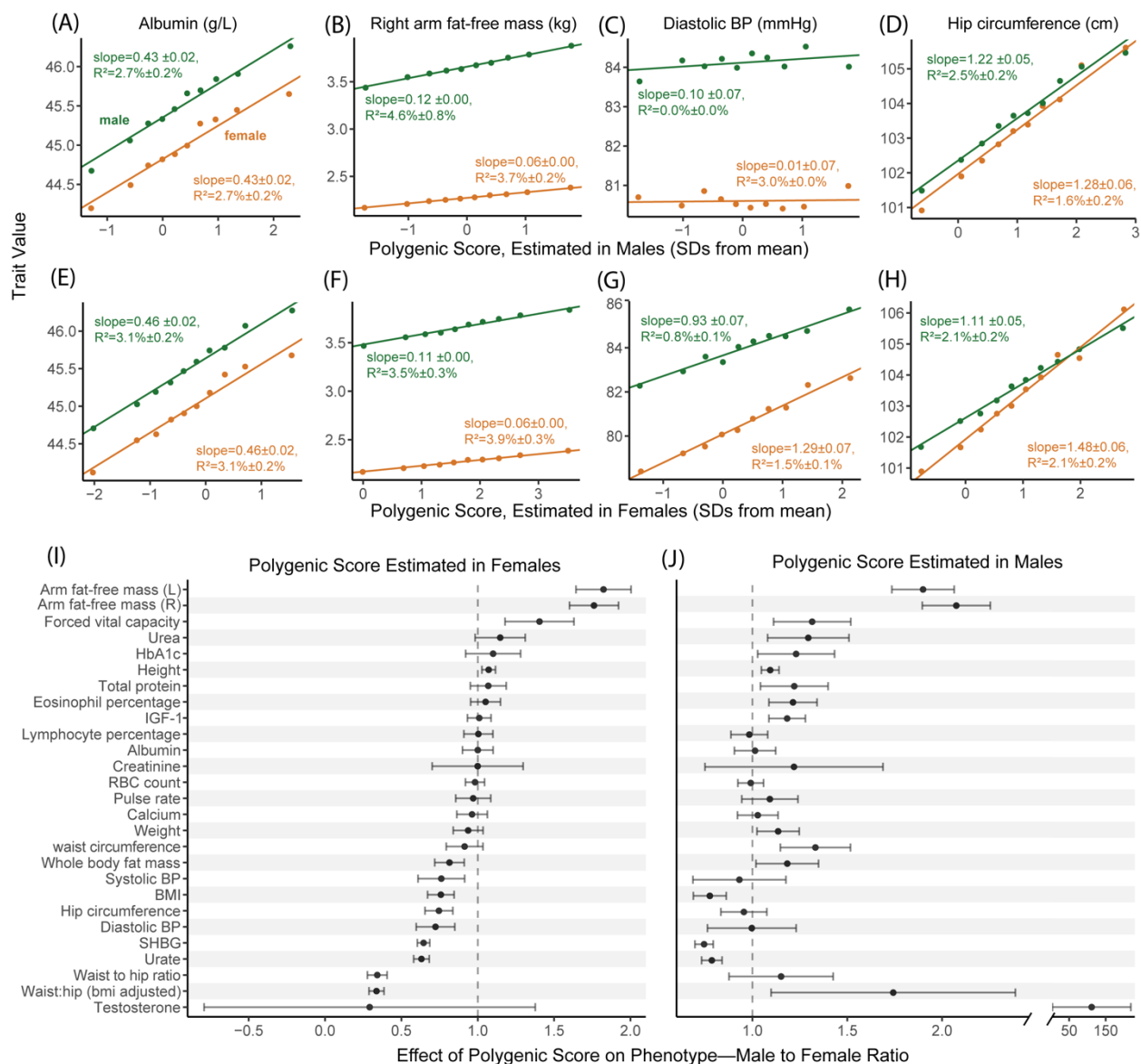
169

Table 1. Polygenic Models of GxSex. We examine different models of the nature of GxSex in complex traits that link to previous studies and motivations. Each model leads to different expectations from the analysis of heritability and genetic correlations (Fig. 1). The illustrations in the third column depict examples of directions and magnitudes of genetic effects, corresponding to each model. h_m^2 , h_f^2 and h^2 denote narrow-sense heritabilities in males, females, and a combined sample, respectively.

discussion in Khramtsova et al.¹⁴). This motivated us to estimate the covariance between genetic effects in males and females directly. Another reason to treat covariance of genetic effects themselves as the estimand of interest is that multiple, distinct GxSex patterns may exist across subsets of genetic factors affecting a trait (Table 1, fourth model).

Flexible model of sex-specific genetic effects as arising from a mixture of covariance relationships.

We set to infer the mixture of covariance relationships of genetic effects among the sexes directly. We analyzed all traits in their raw measurement units as provided by the UKB. In particular, we did not normalize or standardize phenotypes within each sex before performing the sex-stratified GWAS, because sex differences in trait variance may be partly due to amplification. Standardization would have therefore resulted in masking amplification signals that may exist in the data. In some cases, this is indeed the purpose of standardization³⁹. More generally, while each scaling choice has its merits, we view the measurement of genetic effects in their raw units as the most biologically interpretable.



170
 171 **Figure 2: Evaluating evidence for systematic amplification.** (A-D) We regressed trait values in males (green) and
 172 separately in females (orange) on a polygenic score estimated in an independent sample of males. Points show mean
 173 values in one decile of the polygenic score; the fitted line and associated effect estimate and R^2 correspond to
 174 regressions on the raw, non-binned data. In some traits, like Albumin (A), the polygenic score has a similar effect on
 175 the trait in both sexes. In other traits (B,D), the estimated effect of the polygenic score differs significantly, consistent
 176 with a substantial difference in the magnitude of genetic effects of sites included in the polygenic score. (E-H) Same
 177 analysis as A-D, but with a polygenic score pre-estimated in an independent sample of females. (I-J) Summary of the
 178 ratio of the effect of the polygenic score on the trait (± 2 SE) in males to the effect in females across physiological traits.
 179 See results for other traits in **Fig. S12**.

180

181 We used multivariate adaptive shrinkage (*mash*)⁴⁰, a tool that allows the inference of
182 genome-wide frequencies of genetic covariance relationships. Namely, we model the marginal
183 SNP effect estimates as sampled (with SNP-specific, sex-specific noise) from a mixture of zero-
184 centered Normal distributions with various prespecified covariance relationships (2x2 Variance-
185 Covariance matrices for male and female effects; Eq. 1 in Urbut et al.⁴⁰). Our prespecified
186 covariance matrices (“hypothesis matrices”) span a wide array of amplification and correlation
187 relationships, and use *mash* to estimate the mixture weights. Loosely, these weights can be
188 interpreted as the proportion of variants that follow the pattern specified by the covariance matrix
189 (**Fig. 3A**). Our covariance matrices ranged from -1 to 1 in between-sex correlation, and 10 levels
190 of relative magnitude in females relative to males, including matrices corresponding to no effect
191 in one or both sexes (**Fig. S2**).

192 We first focus on testosterone, for which previous research sets the expectation for
193 polygenic male-female covariance. In terms of magnitude, the vast majority of effects should have
194 much greater effect in males. In terms of correlation, we expect a class of genetic effects acting
195 through largely independent and uncorrelated pathways alongside a class of effects via shared
196 pathways¹⁸. Independent pathways include the role of hypothalamic-pituitary-gonadal axis in male
197 testosterone regulation and the contrasting role of the adrenal gland in female testosterone
198 production. Shared pathways involve sex hormone-binding globulin (SHBG), which decreases the
199 amount of bioavailable testosterone in both males and females. As expected, we found that
200 mixture weights for testosterone concentrated on greater magnitudes in males and largely
201 uncorrelated effects. Out of the 32% total weights on matrices with an effect in at least one sex,
202 98% of the weights were placed on matrices representing larger effects in males, including 20.4%
203 ($\pm 0.7\%$) having male-specific effects (**Fig. 3, S5**).

204
205 **Amplification of genetic effects is the primary mode of GxSex.** The only trait of the 27
206 where a large fraction ($\geq 10\%$) of non-zero effects were negatively correlated was testosterone
207 (17%). Most effects were instead perfectly or near-perfectly correlated. For example, diastolic
208 blood pressure and eosinophil percentage had 66% (**Fig. 3**) and 68% (**Fig. S5**) of effects being
209 perfectly correlated, respectively. Overall, the low weights on matrices representing negative
210 correlation do not support opposite directions of effects being a major mode of GxSex (**Fig. S8**).

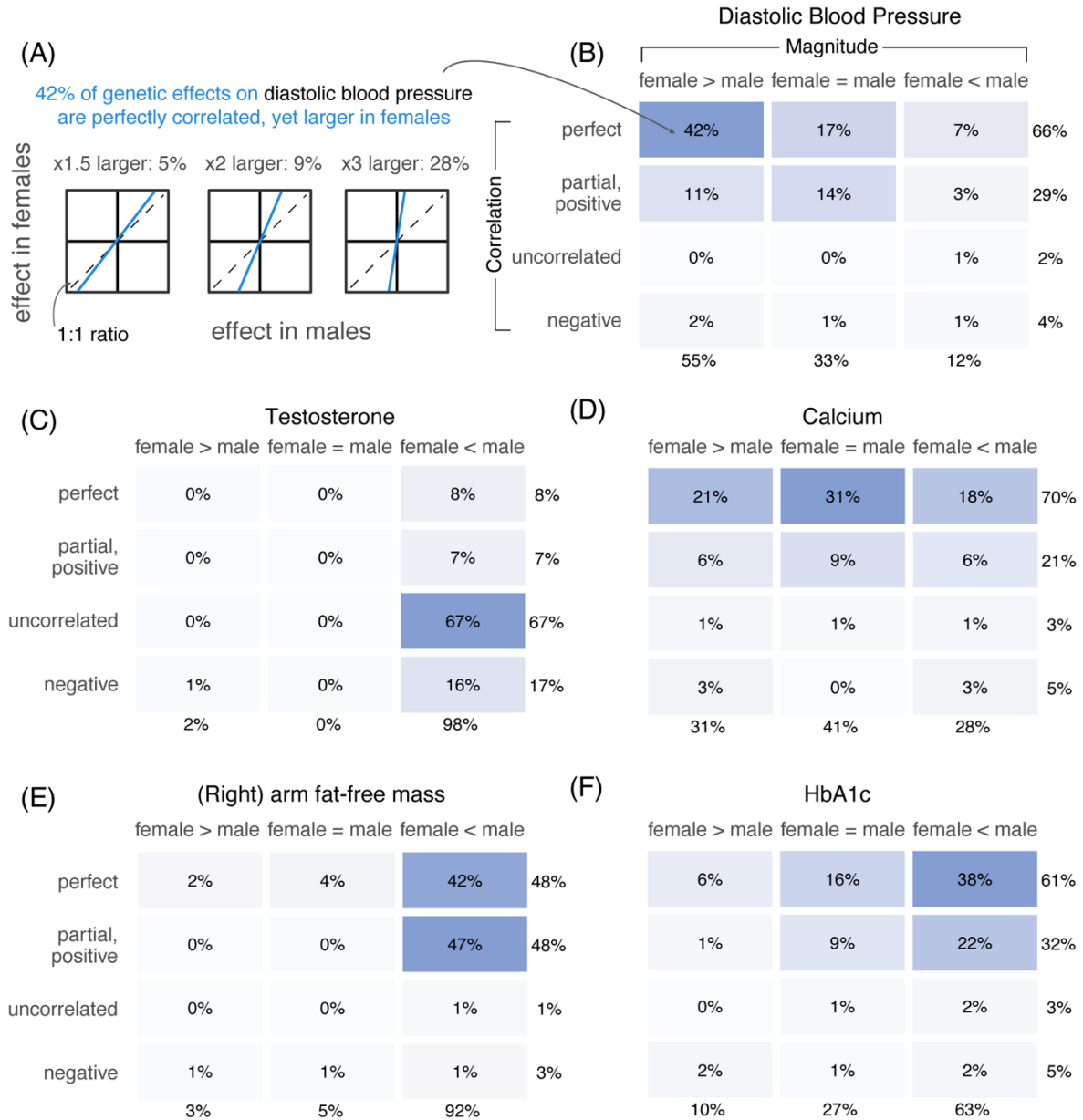
211 In some traits, such as hemoglobin A1C or diastolic blood pressure, previously considered non-
212 sex-specific because of high genetic correlations between sexes and a concordance in top GWAS
213 hits, we find evidence for substantial GxSex through amplification (**Fig. 3B,F; Fig. S5**)^{20,21}.
214 Furthermore, about half (13/27) of the traits analyzed had the majority of weights placed on
215 greater effects in just one of the sexes (x-axis in **Fig. 4A**). For instance, 92% of effects on BMI-
216 adjusted waist:hip ratio were greater in females and 92% of effects on (right) arm fat-free mass
217 were greater in males. Both traits had mixture weights concentrated on highly correlated effects
218 (**Fig. 3**). We confirmed, using a simulation study, that this summary of sex-biased amplification
219 indeed captures sex differences in the magnitude of genetic effects and that it is not due to
220 differences in the extent of estimation noise (e.g., variation in environmental factors independent
221 of genetic effects; **Figs. S6-7; Methods**).

222 Across traits, the difference between the fraction of male-larger effects and the fraction of
223 female-larger effects correlates strongly with male-to-female phenotypic variance ratio (Pearson
224 $r = 0.873$, $p\text{-value} = 6 \cdot 10^{-9}$ after removing testosterone as an outlier; **Fig. 4A**). This observation is
225 consistent with our hypothesis of amplification leading to differences in genetic variance between
226 sexes and thereby contributing substantially to sex differences in phenotypic variance. Together,
227 these observations point to amplification, rather than uncorrelated effects, as a primary mode of
228 polygenic GxSex.

229 Another important question about the implication of pervasive amplification is whether it
230 is a major driver of mean phenotypic differences. The ratio between male and female phenotypic
231 means is correlated with the difference between male-larger and female-larger amplification
232 (Pearson $r = 0.75$; $p\text{-value} = 2 \cdot 10^{-5}$ after removing testosterone and BMI-adjusted waist:hip ratio
233 as outliers). Though this correlation is intriguing, within-sex GWAS aims to explain individual
234 differences from the mean of the sex, and such GWAS results do not dictate the values of the sex
235 means. Further, both the ratio of mean trait values between sexes and the difference in
236 amplification are strongly correlated with phenotypic variance ratios (**Fig. 4A; Fig. S9**; see also
237 Karp et al.⁸), , and many different causal accounts could explain these correlations.

238 Finally, the pervasiveness of GxSex, alongside the mixture of covariance relationships
239 across the genome for many traits, may be important to consider in phenotypic prediction. We
240 compared the prediction accuracy of PGSs that consider the polygenic covariance structure to

Mixtures of covariance relationships of genetic effects between males and females



241

242

243

244

245

246

247

Figure 3: Polygenic covariance structure between males and females. (A) Our analysis of the polygenic covariance between males and females is based on sex-stratified GWAS. We modelled the sex-stratified GWAS estimates as sampled with error from true effects arising from a mixture of possible covariance relationships between female and male genetic effects. As an example, shown are illustrations for three possible relationships of the same qualitative nature—perfectly correlated effects which are also larger in females—and the mixture weights estimated for each in the case of diastolic blood pressure. (B-F) Each box shows the sum of weights placed on all covariance relationships

248 of the same qualitative nature, as specified by relative magnitude (horizontal axis) and correlation (vertical axis)
249 between male and female effects. The full set of pre-specified covariance matrices is shown in **Fig. S2**, and the weights
250 placed on each of them for each trait are shown in **Fig. S5**. All weights shown are percentages of non-null weights, i.e.,
251 the weight divided by the sum of all weights except for the one corresponding to no effect in either sex.

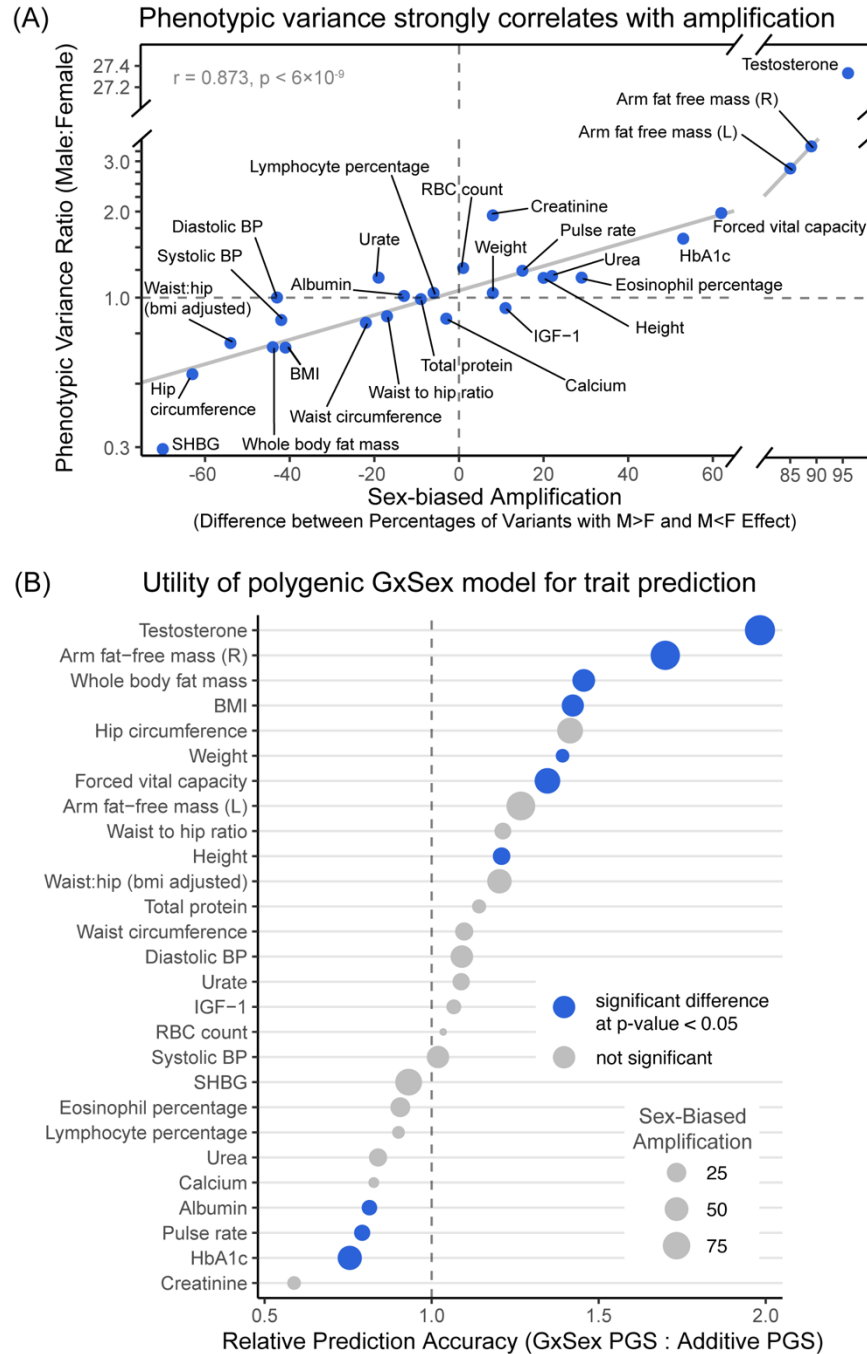
252

253 that of additive models, that ignore GxSex, as well as models that include GxSex but do not
254 consider the polygenic covariance structure (**Supplementary Materials; Fig. S13**). Indeed, for
255 most traits, models that consider the polygenic covariance structure outperform all other models
256 (18/27 traits, $p < 0.05$ for a conservative two-sample $t(1)$ -test for 7/27 traits). Traits which showed
257 better prediction accuracy using the model that considered polygenic covariance structure
258 included many body mass-related traits such as BMI and whole body fat mass that also tended
259 to have higher sex-based amplification (**Fig. 4B**; Pearson $r = 0.62, p < 0.001$ between sex-
260 biased amplification and prediction accuracy ratio). These results point to the utility of considering
261 polygenic covariance structure in context-aware polygenic score prediction.

262

263 **Testosterone as an amplifier.** Thus far, we treated the genetic interaction as discretely
264 mediated by biological sex. One mechanism that may underlie GxSex is a cue or exposure that
265 modulates the magnitude (and less often, the direction) of genetic effects, and varies in its
266 distribution between the sexes. A plausible candidate is testosterone. Testosterone may be a key
267 instigator since the hormone is present in distinctive pathways and levels between the sexes and
268 a known contributor to the development of male secondary characteristics, so therefore could
269 modulate genetic causes on sex-differentiated traits.

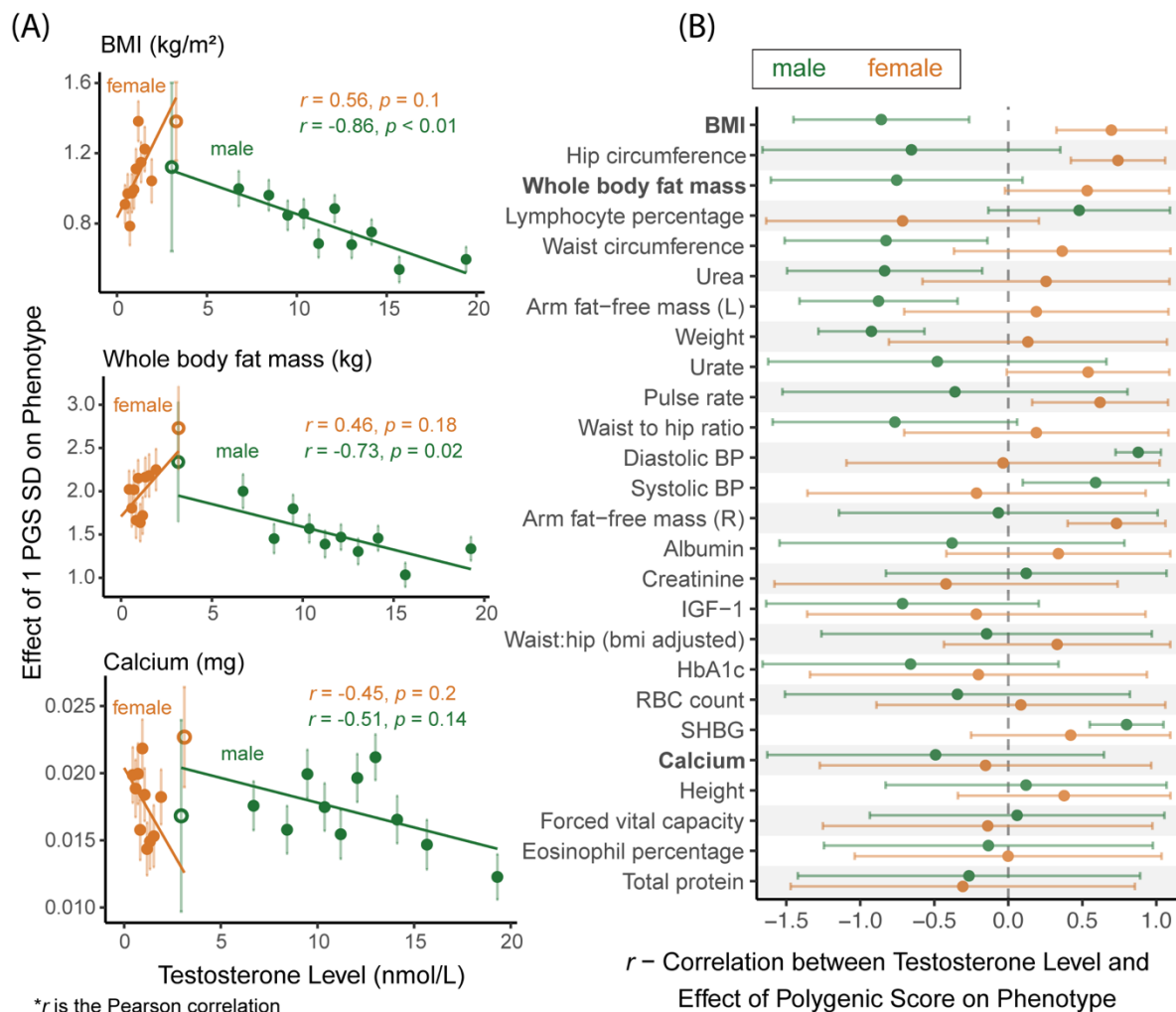
270 To test this idea, we first binned individuals of each sex by their testosterone levels. Then,
271 for each trait and within the bin, we quantified the magnitude of total genetic effect as the linear
272 regression coefficient of trait to a PGS for the trait (**Methods**; see **Fig. S15** for results obtained
273 using sex-specific PGS). For BMI, testosterone (mean per bin) and the magnitude of genetic
274 effect were correlated for both males and females (Pearson p -value < 0.05 ; **Fig. 5A**). For all body-
275 mass-related traits, there was a negative correlation between the magnitude of genetic effect and
276 testosterone levels for males and a positive correlation for females (**Fig. 5B**). Since the
277 relationship with testosterone remains contingent on sex, a model of testosterone as the sole
278 driver of the observed sex-specificity would be invalid. These observations may help explain



279

280 **Figure 4. (A) Phenotypic variance strongly correlates with amplification.** The x-axis summarized the “sex-biased
 281 amplification” of polygenic effects and is calculated by taking the difference between the sum of weights on matrices
 282 with male effects greater in magnitude than female effects (M>F) and the sum of weights of M<F matrices. The solid
 283 gray line shows a linear fit across traits, excluding testosterone as an outlier. **(B) Utility of polygenic GxSex model**
 284 **for trait prediction.** The x-axis shows the relative prediction accuracy estimated from the incremental R² ratio of a

285 GxSex model informed by polygenic covariance patterns and an additive model. The phenotypes are ordered by the
 286 relative prediction accuracy. The size of each point corresponds to the degree of sex-biased amplification as described
 287 in (A). Blue points correspond to traits with a significant difference based on a two-sample t-test with p-value < 0.05
 288 (Text S8) between the covariance-aware GxSex model and the additive model, one way or the other.
 289



290
 291 **Figure 5. Amplification of total genetic effect in relation to testosterone levels.** (A) The relationship between
 292 testosterone level bins and estimated magnitude of genetic effect on traits is shown for three traits. The magnitude of
 293 genetic effect is estimated using the slope of the regression of phenotypic values to polygenic scores in that bin. The
 294 units on the y-axis are effect per standard deviations (SD) of the polygenic scores across all individuals in all bins. The
 295 hollow data points are bins with overlapping testosterone ranges between males and females; these are based on
 296 fewer individuals (~800 compared to ~2200 in other bins) and not included in the regression. Fig. S14 show all other
 297 traits analyzed. (B) The correlation for each sex (90% CI) are shown for all 27 traits. Traits are ordered in descending
 298 order of male-female differences in Pearson correlation.

299 previous reports of positive correlations between obesity and free testosterone in women, and
300 negative correlations in men⁴¹. We conclude that in body-mass related traits, testosterone may
301 be modulating genetic effects in a sexually antagonistic manner.

302 We performed two additional analyses designed to control for possible caveats to the
303 association of testosterone and the magnitude of polygenic effect: An association test that
304 controls for possible confounding with age (**Fig. S17**) and a test that mitigates confounding with
305 other variables or reverse causality (wherein the magnitude of genetic effect affecting the focal
306 trait causally affecting testosterone levels; **Fig. S16**). The evidence for an effect of testosterone
307 on the magnitude of polygenic effect did not remain significant in either of these tests. It is
308 possible, however, that this was due to low statistical power (**Methods**).

309

310 **Are polygenic and environmental effects jointly amplified?** Our results thus far suggest
311 that polygenic amplification across sexes is pervasive across traits; and that the ratio of
312 phenotypic variance scales with amplification (**Fig. 4A**). An immediate question of interest is
313 whether the same modulators that act on the magnitude of genetic effects act on environmental
314 effects as well (see also relevant discussion by Domingue et al.⁴²). Consider the example of
315 human skeletal muscle. The impact of resistance exercise varies between males and females.
316 Resistance exercise can be considered as an environmental effect since it upregulates multiple
317 skeletal muscle genes present in both males and females such as IGF-1, which in turn is involved
318 in muscle growth⁴³. However, after resistance exercise at similar intensities, upregulation of such
319 genes is sustained in males, while levels return sooner to the resting state in females (**Fig. S18**).
320 It is plausible that modulators of the effect of IGF-1, such as insulin⁴⁴ or sex hormones^{45,46}, drive
321 a difference in the magnitude of effect of core genes such as IGF-1 in a sex-specific manner. To
322 express this intuition with a model: If amplification mechanisms are shared, then amplification
323 may be modeled as having the same scalar multiplier effect on genetic and environmental effects
324 (**Fig. 6A**). In the **Methods** section, we specify the details of a null model of joint amplification,
325 which yields the prediction that the male-female ratio of genetic variances should equal the
326 respective ratio of environmental variances (blue line in **Fig 6B**).

327 This expectation is qualitatively different from those of two longstanding theoretical “rules
328 of thumb” predictions for sex differences in trait variance (**Supplementary materials; Fig. S19A**;

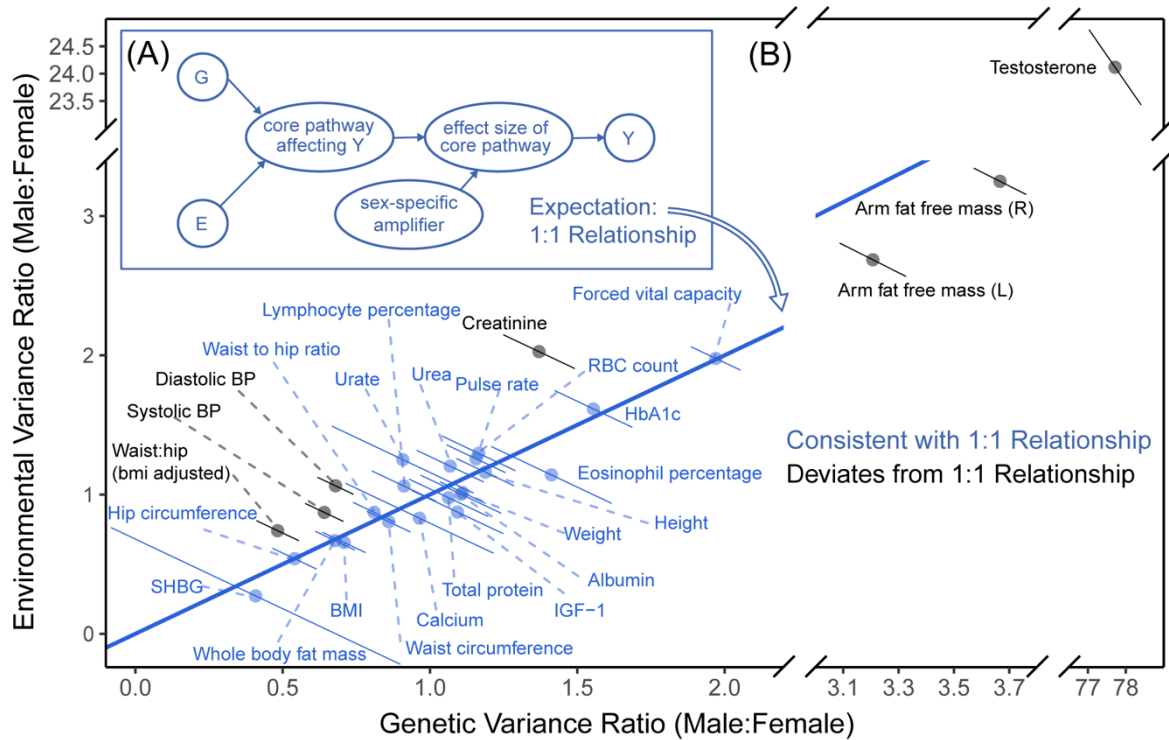
329 of. Zajitschek et al.⁴⁷): The "greater male variability" and "estrus-mediated variability" models,
330 which provide a poor fit across the 27 physiological traits analyzed (**Fig. S19B**).

331 We tested the fit of the theoretical prediction under pervasive joint amplification across
332 traits. We used our estimates of sex-specific phenotypic variance and SNP heritabilities to
333 estimate the ratios of genetic and environmental variances. We note that environmental variance
334 is proxied here by all trait variance not due to additive genetic effects, and caution is advised with
335 interpretation of this proxy. Twenty of the 27 traits were consistent with the null model of pervasive
336 joint amplification (within 90% CI; **Fig. 6B**). This finding may suggest a sharing of pathways
337 between polygenic and environmental effects for these traits (**Fig. 6A**). Interesting exceptions
338 include diastolic blood pressure—which was the strongest outlier ($p\text{-value} = 3.06 \cdot 10^{-12}$, single-
339 sample z-test), excluding testosterone.

340
341 **Sexually antagonistic selection.** A hypothesized cause of sexual dimorphism is sexually
342 antagonistic selection, in which some alleles are beneficial in one sex yet deleterious in the
343 other^{4,5,7,48,49}. Sexually antagonistic selection is difficult to study using traditional population
344 genetics methods because Mendelian inheritance equalizes autosomal allele frequencies
345 between the sexes at conception, thereby erasing informative signals. One way around this
346 limitation is to examine allele-frequency differences between the sexes in the current generation,
347 known as "selection in real time"^{7,50,51}. In this section, we consider a model of sexually antagonistic
348 selection acting on a polygenic trait and use it to estimate the strength of contemporary viability
349 selection acting on the 27 traits we analyzed.

350 Most theoretical models of sexually antagonistic selection on a trait under stabilizing selection
351 usually posit either highly distinct male and female fitness optima or genetic variants affecting
352 traits antagonistically. Our findings on pervasive amplification suggest that variant effects on traits
353 tend to have concordant signs. Yet, under pervasive amplification, a somewhat surprising intuition
354 arises: Alleles affecting a trait may frequently experience sexually antagonistic selection—both in
355 the case in which trait optima for males and females are very distinct (**Fig. 7B**) and for the case
356 in which they are similar (**Fig. 7A**).

357 We developed a theoretical model of sexually antagonistic viability selection on a single
358 trait that builds on this intuition. The model relates sex-specific effects on a complex trait to the
359 divergence in allele frequency between males and females (measured as F_{ST} ^{52,53}) due to viability



360

361 **Figure 6. Testing a model of pervasive, joint amplification of environmental and polygenic effects. (A)** A model
 362 of equal amplification of genetic (G) and environmental (E) effect, that produces the sex differences in the distribution
 363 of the phenotype, Y. G and E both act through a core pathway that is amplified in a sex-specific manner. **(B)** The blue
 364 1:1 line depicts the theoretical expectation under a simple model of equal amplification of genetic and environmental
 365 effects in males compared to females. Error bars show 90% confidence intervals. Traits in blue are consistent (within
 366 their 90% CI) with the theoretical prediction. **Fig. S19** shows the same data alongside the predictions under other
 367 theoretical models of male-female variance ratios.

368

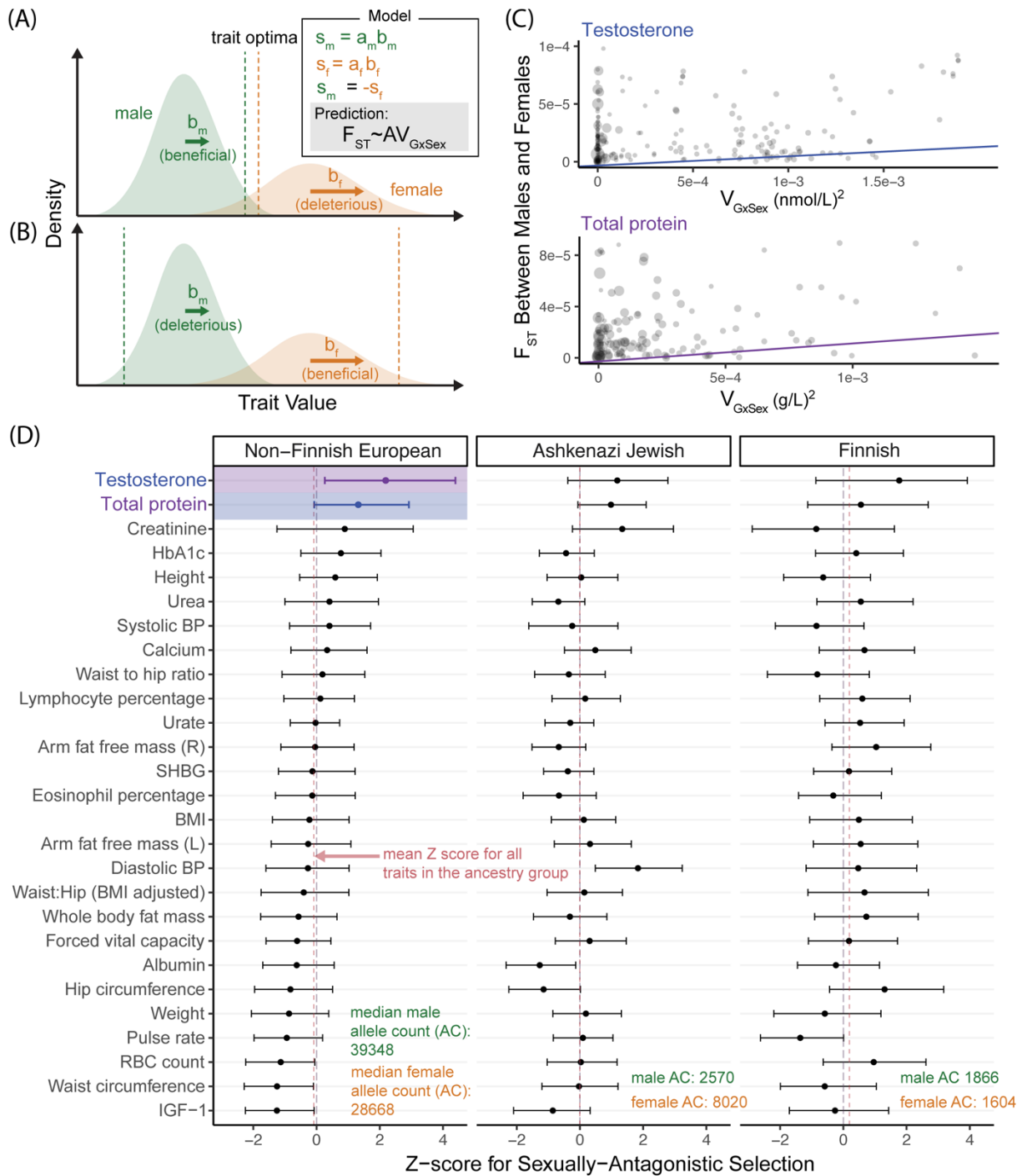
369 selection “in real time”, i.e., acting in the current generation between conception and the
 370 time of sampling. We derive the expected relationship for each site i ,

$$F_{ST_i} \approx AV_{GxS_i} \quad (1)$$

371 where

$$V_{\{GxS\}_i} = 2p_i(1 - p_i)(\beta_i^m - \beta_i^f)^2,$$

372 and p_i , β_i^m and β_i^f are the allele frequency of an allele at site i , its effect on the trait in males and
 373 its effect in females, respectively. A is a constant parameter shared across all variants and can
 374 therefore be interpreted as the effect of sexually antagonistic selection on male-female divergence



375

376 **Figure 7. Testing for sexually antagonistic selection. (A,B)** A model of sexually antagonistic selection. Selection

377 coefficients, s_m and s_f , are linear with the additive effect on the trait in each sex. Sexually antagonistic selection acts

378 such that $s_m = -s_f$. The model yields the prediction of **Eq. 1**. In (A), the effect of an allele tends to drive trait values
379 towards the optimum in males, and away from the optimum in females. In (B), the fitness optima are farther in males
380 and females; in both examples, selection on acts antagonistically (i.e., in opposite directions). **(C)** Two examples of the
381 weighted least-squares linear regression performed to estimate the strength of sexually antagonistic selection on
382 variants associated with a trait (A in panel A and **Eq. 1**). Each point shows one SNP. Size is proportional to each point's
383 regression weight. **(D)** Z-scores (90% non-parametric bootstrap CI) estimated through 1000 resampling iterations of
384 the weighted linear regression of panel B for each trait. The two colored estimates correspond to the examples in (B).

385
386 at variants associated with the trait (**Methods**). We estimated F_{ST_i} for all sites i across subsamples
387 of various ancestry groups in the gnomAD dataset⁵⁴. To estimate $V_{\{GxS\}_i}$ at each site and for each
388 trait, we used our sex-stratified GWAS results. Since there is large heterogeneity in uncertainty
389 of GxSex-genetic variance estimates, we use a variance-weighted linear regression to estimate
390 A (see **Methods** for the derivation of the variance of $V_{\{GxS\}_i}$ estimates and **Supplementary**
391 **Materials** for further details).

392 Recent work has shown that apparent sex differences in autosomal allele frequencies
393 within a sample are often due to a bioinformatic artifact: The mismapping of sequencing reads
394 from autosomes to sex chromosomes or vice versa^{48,55,56}. We identified and excluded sites which
395 are potentially vulnerable to this artifact (**Supplementary Materials**). In **Fig. 7D**, we only show
396 results for gnomAD subsamples that are the closest in their genetic ancestry to our UKB sample⁵⁷
397 (results for other subsamples are shown in **Fig. S20,21**). Furthermore, given the concerns of study
398 recruitment biases^{38,55}, we place higher confidence in results that replicate qualitatively across
399 different subsamples, even though we note that subsample-specific selection signals may be real
400 since sexually antagonistic selection may act heterogeneously across groups.

401 With these conservative criteria considered, we only find evidence for sexually
402 antagonistic polygenic selection on testosterone. In the non-Finnish sample, the largest of the
403 three samples, the null hypothesis $H_0: A = 0$ in **Eq. 1** is rejected (p-value < 0.05) only for
404 testosterone (Z score = 2.2). Testosterone is among the three strongest signals in the two other
405 samples as well, though none of the traits are statistically significant in these samples.

406

407 Discussion

408 Departing from previous studies that sought GxSex through single loci or heritability analyses, we
409 modelled GxSex as a mixture of polygenic relationships across the genome. Our analysis
410 supports pervasive context-dependency of genetic effects on complex traits, acting largely
411 through amplification. Surprisingly, even for some traits such as red blood cell count, previously
412 considered non-sex-specific because of high genetic correlations between sexes and a
413 concordance in top GWAS hits, we find evidence for substantial GxSex. The strong relationships
414 we find between amplification, environmental variance and phenotypic variance further points to
415 its potential importance for sex differences.

416 We have shown that considering the polygenic covariance structure, including
417 amplification signals, improves phenotypic prediction for most traits. Its incorporation in polygenic
418 scores is straightforward. We therefore recommend its broad application and further building on
419 our approach to improve clinical risk stratification and other applications of polygenic scores.

420 Our findings may seem at odds with previous reports of GxSex primarily consisting of sex-
421 limited effects (i.e., no effect in one of the sexes) or antagonistic effects (differences in sign)⁵⁸. In
422 the **Supplementary Materials** and **Table S6**, we illustrate that these apparent discrepancies may
423 be rooted in ascertainment biases. Therefore, limiting analyses to variants with outsized sex
424 differences provides a clouded picture of polygenic GxSex.

425 Localization of GxSex signals can provide clues into the modulators underlying
426 amplification. Here, we proposed one such modulator, testosterone, and found a correlation
427 between testosterone levels and the magnitude of genetic effect on whole body fat mass. The
428 opposite signs of these correlations in females and males may reflect the discrepant relationship
429 between testosterone and these traits at the phenotypic level.

430 Our approach for studying GxSex in complex physiological traits can be adopted to study
431 the moderation of polygenic effects by other environments. Starting out with sex as an
432 environmental variable offers a methodological advantage. The study of context-dependency in
433 humans is often complicated by study participation biases, leading to genetic ancestry structure
434 that confounds genotype-phenotype associations^{38,59-61}, reverse causality between the
435 phenotype and environment variable, collider bias, gene-by-environment correlation and other
436 problems⁶²⁻⁶⁴. Focusing on sex as a case study circumvents many of these “usual suspects”
437 problems: For example, problems involving the phenotype causally affecting sex are unlikely. This

438 is an important benchmark for future studies of environmental modulation, both because of the
439 methodological advantage of sex as an environmental variable and because sex is almost always
440 measured; so insight into sex differences in genetic effects can be incorporated straightforwardly
441 in future studies and in clinical risk prediction. Here, we showed that for most of the traits
442 considered, modeling polygenic GxSex (as opposed to individually estimating sex-specific effects
443 at each site; **Fig. S13** yields sex-specific predictors that outperform standard additive polygenic
444 scores.

445 Finally, we developed a model to consider how GxSex may fuel sexually antagonistic
446 selection in contemporary populations. Over long evolutionary timescales, the two scenarios
447 depicted in **Fig. 7A,B** may lead to different predictions about the long-term maintenance of GxSex
448 genetic variance. Regardless, in both cases, alleles that underlie GxSex may experience sexually
449 antagonistic selection.

450 We found suggestive signals of sexually antagonistic selection on variation associated
451 with testosterone levels (also see related results by Ruzicka et al.⁵¹). The signal for our inference
452 of selection is systematic allele frequency differences between adult males and females, which
453 are consistent with contemporary viability selection. The severity, age of onset and prevalence of
454 nearly all diseases are sexually dimorphic⁶⁵. These signals may therefore point to a related
455 disease that differentially affects lifespan in the two sexes, such as immune system suppression,
456 diabetes, cancers, and hypertension⁶⁶⁻⁶⁹. Recently, high testosterone levels have been linked to
457 increased rates of mortality and cancer in women, but decreased rates in men^{70,71}. However, the
458 testosterone result is also consistent with other accounts, such as testosterone having opposing
459 effects on propensity to participate in a study in the two sexes. Further validation is therefore
460 required to better test hypotheses of sexually antagonistic selection, for example in studies with
461 no recruitment biases (or at least distinct recruitment biases).

462 In this work, we have shown that amplification of the magnitude of polygenic effects may
463 be important to consider as a driver of sex differences and their evolution. Our approach included
464 the flexible modelling of genetic effect covariance among the sexes, as well as various
465 subsequent analyses exploring the implications of these covariance structures. We hope this
466 study can inform future work on the context-specificity of genetic effects on complex traits.

467

468 **Limitations of the Study**

469 Study participation in large biobanks like the UK Biobank (UKB) differs by sex⁷²; and work by
470 Piratsu et al. further argued that allele frequency differences between males and females may
471 reflect sex-specific recruitment biases⁵⁵. However, a recent study by Benonisdottir and Kong
472 found no evidence of sex-specific genetic associations with UKB participation³⁸, and another by
473 Kasimatis et al. showed that many apparent associations of autosomal genotypes and biological
474 sex in the UKB were instead primarily due to a bioinformatic artifact—the mis-hybridization of
475 autosomal genotyping probes with sex chromosomes⁴⁸. Even still, subtle recruitment biases
476 affecting male and female participation differently remain a possible caveat to our conclusions.
477 For the analysis of natural selection in particular, while the replication of signals of selection in
478 multiple samples may lend credence to our inference, medical datasets based on recruitment of
479 participants via referring physicians, participation biases may still plausibly be shared across
480 studies.

481

482 **Acknowledgments**

483 We thank the Harpak Lab and Edge Lab members, Ziyue Gao, Tom Juenger, Jonathan Pritchard,
484 Molly Przeworski, Guy Sella, Jeff Spence and Elliot Tucker-Drob for helpful comments on the
485 manuscript. We also thank Brian Dilkes, Andrés Bendesky and Jim Fleet for insightful
486 discussions. We thank Abin Abraham and Tony Capra for their help in implementing code from
487 Kasimatis et al.⁴⁸, and Michelle Traglia and Lauren Weiss for useful discussions of the relationship
488 between the results reported here and Traglia et al.⁵⁸. This work was supported by NIH
489 GM116853-07 to M.K. and NIH GM137758 to M.D.E. This study has been conducted using the
490 UK Biobank resource under application Number 61666, as approved by the University of Texas
491 at Austin Institutional Review Board, protocol 2019-02-0125.

492 **Author Contributions**

493 C.Z., M.J.M. and A.H. designed the experiments. C.Z. and M.J.M. performed the experiments.
494 C.Z., M.J.M. and A.H. wrote the paper with assistance from all authors. J.M.C., M.D.E and M.K.
495 provided expertise and feedback.

496 **Declaration of Interests**

497 The authors declare no competing interests.

498 **Methods**

499 **RESOURCE AVAILABILITY**

500 **Lead contact**

501 Further information and requests for resources should be directed to and will be fulfilled by the
502 lead contact, Arbel Harpak (arbelharpak@utexas.edu)

503

504 **Materials availability**

505 This study did not generate new unique reagents.

506

507 **Data and code availability**

508 This study used genotype and phenotype data from the UK Biobank
509 <https://www.ukbiobank.ac.uk/>.

510 Sex-specific GWAS summary statistics are available at Zenodo and are publicly available as of
511 the data of publication. DOIs are listed in the key resources table.

512 All original code has been deposited at https://github.com/harpak-lab/amplification_gxsex and is
513 publicly available as of the date of publication. DOIs are listed in the key resources table.

514 Any additional information required to reanalyze the data reported in this paper is available from
515 the lead contact upon request.

516

517 **METHOD DETAILS**

518 **UK Biobank sample characteristics.** The UK Biobank is an extensive database that
519 contains a wide variety of phenotypic and genotypic information of around half a million
520 participants aged 40-69 at recruitment⁷³.

521 In this study, we considered 337,111 individuals who passed quality control (QC) checks,
522 which included the removal of samples identified by the UK Biobank with sex chromosome
523 aneuploidy or self-reported sex differing from sex determined from genotyping analysis. We
524 excluded related individuals (3rd-degree relatives or closer) as identified by the UK Biobank in
525 data field 22020. To reduce potential population structure confounding, we further limited our
526 sample to individuals identified by the UK Biobank as “White British” in data field 22006. These

527 are individuals who both self-identified as White and as British and were additionally very tightly
528 clustered in the genetic principal component space^{73,74}. Individuals who had withdrawn from the
529 UK Biobank by the time of this study were removed. For each phenotype, we also removed
530 individuals who had missing data for the specified phenotype. These procedures left us with
531 between 255,426 to 336,551 individuals in the analysis for each trait.

532

533 **Expectations for sex-specific heritabilities with no GxSex.** In the section “The limited
534 scope of analyzing GxSex via heritability differences and genetic correlations,” we report our
535 observation that, for most traits examined, sex-specific heritabilities (i.e., estimated independently
536 from sex-stratified GWAS) were both higher than the heritability in the combined sample. Here,
537 we explain why this observation is inconsistent with a simple model in which genetic effects are
538 the same across the sexes.

539 Under a simple additive model of variance in a trait Y within each sex Z ,

$$\text{Var}[Y|Z] = \text{Var}[G|Z] + \text{Var}[E|Z], \quad (2)$$

540 where Y, G, E represent the trait value, additive effect, and environmental effect (including all non-
541 genetic context aside from sex), respectively. Under this model, the sex-specific heritability h_z^2 is

$$h_z^2 = \frac{\text{Var}[G|Z]}{\text{Var}[G|Z] + \text{Var}[E|Z]}. \quad (3)$$

542 Therefore, sex differences in heritability are either due to sex differences in genetic
543 variance, in environmental variance, or both. If genetic effects are equal, differences in
544 environmental variance alone could cause heritability differences (**Table 1**, first model). But as
545 we show below, the heritability in the combined sample cannot be smaller than both sex-specific
546 heritabilities.

547 We assume as before that allele frequencies are highly similar between males and
548 females. Since genetic effects are equal, this implies

549
$$\text{Var}[G|Z = m] \approx \text{Var}[G|Z = f].$$

550 For the environmental variance, we have that

$$\text{Var}[E] = \mathbb{E}_Z[\text{Var}[E|Z]] + \text{Var}_Z[\mathbb{E}[E|Z]] = \mathbb{E}_Z[\text{Var}[E|Z]] + 0 = \quad (4)$$

$$\mathbb{P}(Z = m)\text{Var}[E|Z = m] + \mathbb{P}(Z = f)\text{Var}[E|Z = f] \leq \max_{z \in \{m, f\}} \text{Var}[E|Z = z].$$

551 The first equality follows from the law of total variance. In the second equality, we have
552 assumed that there are no mean sex differences in the environmental effects (or, in practice in
553 our analysis and as routine in other analyses, that mean phenotypic sex differences have been
554 subtracted out), giving

$$555 \mathbb{E}[E|Z = m] = \mathbb{E}[E|Z = f] = \mathbb{E}[E].$$

556 **Eq. 4** shows that the combined environmental variance cannot be greater than the larger of the
557 two sex-specific environmental variances. It follows that if the genetic variance is equal in both
558 sexes, then the heritability in the combined sample cannot be smaller than both of the sex-specific
559 heritabilities,

$$h^2 = \frac{\text{Var}[G]}{\text{Var}[G] + \text{Var}[E]} \geq \frac{\text{Var}[G]}{\text{Var}[G] + \max_{z \in \{m, f\}} \text{Var}[E|Z]} = \min_{z \in \{m, f\}} h_z^2. \quad (5)$$

560
561 **Multivariate adaptive shrinkage (mash).** We used multivariate adaptive shrinkage (*mash*) to
562 examine correlation and differences in magnitude of SNP effects between males and females⁴⁰.
563 *mash* is an adaptive shrinkage method⁷⁵ that improves upon previous methods of estimating and
564 comparing effects across multiple conditions by flexibly allowing for a mixture of effect covariance
565 patterns between conditions and requiring only summary statistics from each condition (including
566 a point estimate of the effect and corresponding standard error for each SNP and condition). The
567 method adapts to patterns of sparsity, sharing, and correlation among the conditions to compute
568 improved effect estimates.

569 In this study, we set two conditions, male and female, and provided effect estimates and
570 corresponding standard errors from our male-specific and female-specific GWAS. *mash* learns
571 from the data by estimating mixture proportions of various predefined covariance matrices
572 representing different patterns in effects. Using maximum likelihood, *mash* assigns low weights
573 to matrices that capture fewer patterns in the data, and higher weights to those that capture more.

574
575 **Mixture weights for covariance structure between male and female effects.** To interpret
576 patterns of SNP effects between males and females, we inputted 66 hypothesis-based covariance

577 matrices (**Fig. S2**) spanning a range of correlations and relative magnitudes of effects between
578 males and females. We used a random subset of all SNPs for *mash* to learn the covariance
579 mixture weights. In order for the random subset to contain approximately independent SNPs and
580 capture the weight of SNPs with no effect (**Fig. S2**), we created a subset of SNPs for each trait
581 by taking a random SNP from each of 1703 approximately independent LD blocks estimated for
582 Europeans⁷⁶. *mash* can also generate data-driven covariance matrices that capture SNP effects
583 in the data, but we did not use this feature since the data-driven matrices had negligible
584 differences from our hypothesized matrices (in terms of ℓ_2 norm) and were less interpretable.
585 For each trait, we repeat this weight-learning step 100 times, sampling the SNPs from the 1703
586 LD blocks without replacement to fit the *mash* model and generate mixture proportions. We then
587 take the average proportion for each covariance matrix as an estimate of its weight, effectively
588 treating each of the 100 samples as i.i.d. draws.

589

590 **Choice of SNPs used to estimate male-female effect covariance.** We examined the
591 effect of using a random subset taken from different p-value thresholds [1, 5e-2, 1e-5, 5e-8] while
592 selecting from LD blocks. By doing so, we can examine differences in the distribution of weights
593 across the p-value thresholds. We performed this test on height, BMI, testosterone, and BMI-
594 adjusted waist:hip ratio. For each trait, weight placed on the no-effect matrix decreased as we
595 reduced the p-value threshold (**Fig. S4A**). Patterns of weights for non-null effect matrices varied
596 across the traits (**Fig. S4B,C**). Since *mash* considers the proportion of null effects and sex-
597 specific, SNP-specific noise; together with the fact that for complex traits, less significant
598 associations may still reflect valuable signal, we decided on using the whole set of SNPs to
599 sample from when estimating mixture proportions.

600

601 **Simulating equal genetic effects and heterogeneous estimation noise among the sexes.**

602 To ensure that *mash* was not mistaking sex differences in estimation noise (e.g. via
603 differences in the extent of environmental variance) to be differences in the magnitude of genetic
604 effects, we performed a simulation study. In short, samples of males and females were generated
605 under the model given by **Eq. 2**. Genetic effects were set as equal, but the environmental variance
606 differed among the sexes. We then perform a GWAS on both samples and input the simulated
607 GWAS results into *mash*, and test whether the estimated mixture weights spuriously suggest the

608 presence of GxSex. We performed this simulation on a grid of parameters, including heritabilities
609 in males set to either 5% or 50%, female to male environmental variance ratio of 1, 1.5 or 5; and
610 100, 1,000 or 10,000 causal SNPs.

611 First, we created a sample of 300K individuals with randomly assigned sex. We then
612 sampled genotypes for all individuals consisting of 20K SNPs by sampling from the observed
613 distribution of allele frequencies from UK Biobank's imputed data⁷⁷, assuming linkage equilibrium.
614 From the 20K SNPs, we portioned out the predetermined number of causal SNPs and assigned
615 effect sizes by sampling from a Standard Normal distribution. We estimated the male
616 environmental variance for each causal SNP using the equation,

$$Var[E|Z = m] = \frac{Var[G|Z = m](1 - h_m^2)}{h_m^2} = \frac{(\sum_{i=0} \beta_i^2 2p_i(1 - p_i))(1 - h_m^2)}{h_m^2} \quad (6)$$

617 where $Var[E|Z = m]$ is the simulated environmental variance for males, $G|Z = m$ is a vector of
618 the genetic effects in males, h_m^2 is the heritability in males and β_i and p_i are the effect size and
619 allele frequency at site i , which are equal for males and females. We multiplied $Var[E|Z = m]$
620 by the predetermined environmental variance ratio to obtain the environmental variance for
621 females $Var[E|Z = f]$. Afterwards, for each individual j with sex z_j , we sampled the
622 environmental effect E_j as

$$E_j \sim N(0, Var[E|Z = z_j]).$$

623 Phenotypes were then set using the following additive model,

$$y_j = \sum_{i=0} \beta_i x_{ij} + E_j \quad (7)$$

624 where y_j is the phenotypic value for individual j and x_{ij} is the number of effect allele copies at the
625 i^{th} causal SNP for the j^{th} individual. With the phenotype, genotype and environmental effect set,
626 we obtained the estimated effect sizes, $\{\hat{\beta}_i\}$, using least squares simple linear regression for all
627 20K SNPs and used the estimated effect sizes and corresponding standard errors as input into
628 *mash*.

629 For nearly all parameters, out of the weights on matrices other than the null matrix, the
630 vast majority was placed on the matrix for perfect correlation, equal magnitude (**Fig S6**). As the
631 number of causal SNPs increased, the weight on the no-effect covariance matrix decreased

632 accordingly. These results suggest that *mash* was not grossly mistaking differences in
633 environmental variance as amplification.

634

635 **Simulating sex-biased amplification.** To evaluate whether *mash* accurately
636 captures sex-biased amplification of genetic effects (a measure we have used in the x-axis of **Fig.**
637 **4A,B**), we followed the same simulation procedure described in the Section "Simulating equal
638 genetic effects and heterogeneous estimation noise among the sexes". However, instead of using
639 equal genetic effects in males and females, we sampled genetic effects from pre-specified
640 covariance matrices (**Fig. S7** left-hand panel). We set the female to male environmental variance
641 ratio as 1.2 and the heritability as 0.5. We generated data from (A) a model in which all genetic
642 effects are sampled from a matrix where male and female effects are equal, (B) a model in which
643 86% of the genetic effects are sampled from a matrix where effects between the sexes are equal,
644 and 14% of the effects are sampled from a matrix where the female effect size magnitude is 4
645 times that of males, and (C) a model in which 86% of effects are sampled from a matrix where
646 effects between sexes are equal, and 14% of effects are sampled from a matrix of only female-
647 specific effects. After simulating sex-specific GWAS on the three models, we input the results into
648 *mash* to estimate mixture weights. We repeated this simulation procedure 100 times for each
649 model.

650 For model (A), the equal effect matrix received 78% of the weight, and the difference
651 between male-larger and female-larger magnitude was 1% (**Fig. S7**). For model (B), 67% of the
652 weight was placed on the matrix for equal effects. The weight difference between male-larger and
653 female-larger magnitude was 13%. In model (C), 69% of the weight was on the matrix for equal
654 effects, and the difference between male-larger and female-larger magnitude was 16%. These
655 simulation results therefore suggest some overestimation of the proportion of SNPs with
656 magnitude differences. However, the measure of "sex-biased amplification" matched that of the
657 pre-specified generative models up to an error of 2%. Therefore, the simulations suggest "sex-
658 biased amplification" is measured accurately in our estimation procedure.

659

660 **Testosterone as an amplifier.** We tested a model of testosterone as a modulator of
661 magnitude differences in males and females. We first split individuals by sex and for each sex,
662 created 10 bins of testosterone levels. We adjusted one of the 10 bins to have testosterone levels

663 overlap between males and females. The overlapping testosterone bin was based on fewer
664 individuals (~800) compared to the other bins (~2200). For each trait, each of the sexes, and
665 within each bin, we performed a simple linear regression of trait values to the PGS for the trait
666 (using a PGS based on both-sex summary statistics (**Supplementary Materials**)). We interpret
667 the estimated coefficient for the effect of the PGS as a proxy for the magnitude of polygenic effect.
668 Finally, we summarized the relationship between testosterone level and magnitude of polygenic
669 effect across bins using the Pearson correlation between the two.

670 To mitigate the possible effects of confounding (of testosterone and magnitude of
671 polygenic effect) or reverse causation (the magnitude of polygenic effect on the focal trait causally
672 affecting testosterone levels) we employed a version of Mendelian Randomization^{78,79} of the same
673 analysis (**Fig. S16**). Namely, we replaced testosterone levels of each individual with their PGS for
674 testosterone. Here, given the near-zero genetic correlation between males and females, we used
675 our sex-specific PGS for each sex; otherwise, the analysis is unchanged.

676 We also examined whether participants' age may have confounded the relationship
677 between testosterone and polygenic effect. In this analysis, instead of using the polygenic effect
678 as the response variable across bins, we used the polygenic effect residualized for mean age in
679 the bin and examined the effect of an individual's polygenic score on the residual (**Fig. S17**).

680

681 **Model of Shared Amplification.** Here, we suggest a null model in which amplification is
682 shared between genetic and environmental effects. We then suggest a prediction that the model
683 yields and explain how we tested this prediction across traits (**Fig. 6**).

684 If an amplifier is shared, it may be modeled as having the same scalar multiplier effect on
685 genetic and environmental effects. Consider the within-sex additive model of **Eq. 1** in the section
686 "The limited scope of analyzing GxSex via heritability differences and genetic correlations" above.
687 For a phenotype value Y_z in sex $z \in \{m, f\}$

$$Y_z = c + G_z + E_z, \quad (8)$$

688 Where c is a constant, E_z is the environmental effect and

$$G_z = \sum_{site\ i} x_i \beta_i^z \quad (9)$$

689 is the polygenic effect where β_i^z is the effect of an allele at site i (say the minor allele) in sex Z
690 and x_i is the number of copies of the allele. We assume here for simplicity that male genetic
691 effects relate to female effects solely through a shared polygenic amplification constant, α ,

$$\beta_i^m = \alpha\beta_i^f \quad \forall i; \alpha > 0. \quad (10)$$

692 Allele frequencies are once again assumed to be close to equal between males and
693 females, since due to random segregation of alleles during meiosis, genotype frequencies at
694 autosomal sites are independent of sex; and further assuming no substantial interaction between
695 genotype and sex affecting participation in UKB³⁸. Consequently, differences in polygenic effect
696 distributions between males and females are solely based on GxSex, and thus:

$$\text{Var}[G_m] = \alpha^2 \text{Var}[G_f]. \quad (11)$$

697 The model we would like to test is one where the amplification of environmental effects
698 can also be simplified to the same scalar multiplier,

$$\begin{aligned} E_m &= \alpha E_f, \text{ and} \\ \text{Var}[E_m] &= \alpha^2 \text{Var}[E_f]. \end{aligned} \quad (12)$$

699 Hence, with equal amplification,

$$\frac{\text{Var}[G_m]}{\text{Var}[G_f]} = \frac{\text{Var}[E_m]}{\text{Var}[E_f]} \quad (13)$$

700

701 To test the model of shared amplification between environmental and polygenic effects
702 (**Eq. 8**) we obtained the genetic and environmental variance for males and females based on the
703 following relationships,

$$\text{Var}[G_z] = h^2 \text{Var}[Y_z] \quad (14)$$

704 and

$$\text{Var}[E_z] = (1 - h^2) \text{Var}[Y_z], \quad (15)$$

705 where $\text{Var}[G_z]$, $\text{Var}[E_z]$, and $\text{Var}[Y_z]$ are the additive genetic, environmental, and phenotype
706 variances, respectively. Estimates of the sex-specific heritabilities, h_z^2 , were obtained from
707 previous estimates using LD Score Regression (**Supplementary Materials**).

708 Representing male genetic or environmental variance as x , and the corresponding female
 709 variance as y , we derived standard errors for the ratio of male to female variance using the 2nd-
 710 order Taylor approximation for the standard error of a ratio of estimators of x and y ,

$$SE\left[\frac{\hat{x}}{\hat{y}}\right] = \sqrt{\text{Var}\left[\frac{\hat{x}}{\hat{y}}\right]} \cong \frac{E[\hat{x}]}{E[\hat{y}]} \sqrt{\frac{\text{Var}[\hat{x}]}{E[\hat{x}]^2} + \frac{\text{Var}[\hat{y}]}{E[\hat{y}]^2} - \frac{2\text{Cov}[\hat{x}, \hat{y}]}{E[\hat{x}]E[\hat{y}]}} \approx \frac{\hat{x}}{\hat{y}} \sqrt{\frac{SE[\hat{x}]^2}{\hat{x}^2} + \frac{SE[\hat{y}]^2}{\hat{y}^2}} \quad (16)$$

711 assuming independence between \hat{x} and \hat{y} since they are statistics of independent sampling
 712 distributions (independent samples of males and females). The standard errors of the genetic and
 713 environmental variance were estimated using the law of total variance for a product of two random
 714 variables. For \hat{a} and \hat{b} , unbiased estimators of the two parameters a and b , respectively, we get

$$SE[\hat{a}\hat{b}] = \sqrt{SE[\hat{a}]^2 SE[\hat{b}]^2 + E[\hat{a}]^2 SE[\hat{b}]^2 + E[\hat{b}]^2 SE[\hat{a}]^2}.$$

715 Plugging in the point estimate \hat{a} for $E[\hat{a}] = a$ and the point estimate \hat{b} for $E[\hat{b}] = b$,

$$\widehat{SE}[\hat{a}\hat{b}] = \sqrt{SE[\hat{a}]^2 SE[\hat{b}]^2 + \hat{a}^2 SE[\hat{b}]^2 + \hat{b}^2 SE[\hat{a}]^2}. \quad (17)$$

716 In this case, a represents the phenotypic variance, and b represents either h_z^2 for
 717 estimation of genetic variance or $(1 - h_z^2)$ for estimation of environmental variance. Lastly, to
 718 obtain the standard error of the phenotypic variance, we used bootstrapping with 100 samples
 719 (with replacement) of estimates of the phenotypic variance in sex z ,

$$\widehat{SE}[\hat{a}] = \sqrt{\frac{\sum_{i=1}^{100} (\text{Var}[Y]_i - \widehat{\text{Var}}[Y_z]_i)^2}{100 - 1}}$$

720 Finally, for each trait, we estimated \bar{Z} , the ratio of the two male-female ratios
 721 (environmental and genetic, y and x axes in **Fig. 6**, respectively), and its standard error, $SE[\bar{Z}]$,
 722 using the same method as in **Eq. 16**. Under the null hypothesis of equal environmental and
 723 genetic amplification (**Eq. 8**),

$$H_0: E[Z] = 0, \quad (18)$$

724 where

$$Z = \frac{\bar{Z} - 1}{SE[\bar{Z}]}.$$

725 In **Fig. 6**, we approximated 90% confidence intervals on Z by treating it as a Z score, i.e.,
726 further treating Z as a Standard Normal.

727

728 **A Model of Sexually antagonistic Selection.** We developed a model relating sex
729 differences in additive effects on a trait at a biallelic locus (β_m and β_f) and divergence in allele
730 frequencies. Our model resembles that of Cheng and Kirkpatrick⁷ who developed a similar model
731 relating allele-frequency differences and sex bias in gene expression. In short, we modelled
732 sexually antagonistic, post-conception viability selection on a focal complex trait. We assumed
733 allele frequencies in adult males, p_m , and adult females, p_f , are at equilibrium, i.e. do not change
734 in consecutive generations. Under these conditions, we derive the relationship

$$F_{ST} \approx AV_{GxSex},$$

735 where F_{ST} ⁵² is the fixation index with respect to the male and female subpopulations, i.e., the
736 proportion of heterozygosity in the population that is due to allelic divergence between the sexes.
737 V_{GxSex} is defined as

$$V_{GxSex} := 2p(1-p)(\beta_m - \beta_f)^2, \quad (19)$$

738 where p is the allele frequency in zygotes. A is a parameter that, importantly, is shared across all
739 variants affecting the trait and can be thought of as the intensity of sexually antagonistic selection
740 acting on genetic variation for the trait in question.

741 In our model, allele frequencies at the autosomal locus are assumed to be equal in males
742 and female zygotes. F_{ST} at adulthood takes the form

$$F_{ST} := \frac{\text{Var}_z[p_z]}{\bar{p}(1-\bar{p})} = \frac{E[p_z^2] - \bar{p}^2}{\bar{p}(1-\bar{p})} = \frac{p_m^2 + p_f^2 - \left(\frac{p_m + p_f}{2}\right)^2}{\bar{p}(1-\bar{p})} = \frac{(p_m - p_f)^2}{4\bar{p}(1-\bar{p})}, \quad (20)$$

743 where

$$\bar{p} = \frac{p_m + p_f}{2}.$$

745 If we further assume a near-1:1 sex ratio such that $\bar{p} \approx p$,

$$F_{ST} \approx \frac{(p_m - p_f)^2}{4p(1-p)}. \quad (21)$$

746 Sexually antagonistic selection acting on viability will cause divergence in allele
747 frequencies between adult males and females. We write the relative viabilities of the homozygote
748 for the reference allele, the heterozygote and the homozygote for the effect allele as $1 :: 1 +$

749 $d_z S_z :: 1 + S_z$ for each sex $z \in \{m, f\}$. The selection coefficient S_z and dominance coefficient d_z
 750 can be frequency-dependent, in which case these coefficients take their values at equilibrium. We
 751 can write the additive selection coefficient of the effect allele as

$$s_z = [p + (1 - 2p)d_z]S_z. \quad (22)$$

752 Assuming that zygotes are at Hardy-Weinberg equilibrium, the allele frequency in each
 753 sex at adulthood is

$$p_z \approx p + p(1 - p)s_z, \quad (23)$$

754 where we neglected terms of order s_z^2 ⁸⁰. Plugging **Eq. 23** into **Eq. 21**, the divergence between
 755 males and females post-selection is

$$F_{ST} \approx \frac{1}{4}p(1 - p)(s_m - s_f)^2. \quad (24)$$

756 We model the strength of viability selection acting on males and females as linear with the
 757 additive effect on a focal trait in each sex,

$$s_z = a_z \beta_z, \quad (25)$$

758 and recalling the simplifying assumption that allele frequencies are at equilibrium under sexually
 759 antagonistic viability selection at the locus, such that selection favoring an allele in one sex is
 760 balanced by selection against that allele in the other sex,

$$s_f = -s_m. \quad (26)$$

761 If $\beta_m = \beta_f$, then **Eq. 24** simplifies to

$$F_{ST} \approx p(1 - p)(a_f \beta_f)^2 = \frac{a_f^2}{2} V_G. \quad (27)$$

762 where

$$V_G = 2p(1 - p)\beta_f^2. \quad (28)$$

763 is the additive genetic variance. However, when β_m does not strictly equal β_f , **Eq. 25, 26** together
 764 imply

$$\beta_m + \beta_f = \frac{\beta_m + \beta_f}{\beta_m - \beta_f} (\beta_m - \beta_f) = \frac{\frac{s_m}{a_m} - \frac{s_m}{a_f}}{\frac{s_m}{a_m} + \frac{s_m}{a_f}} (\beta_m - \beta_f) = \frac{a_f - a_m}{a_f + a_m} (\beta_m - \beta_f). \quad (29)$$

765 Finally, using **Eq. 25**,

$$s_m - s_f = a_m \beta_m - a_f \beta_f = \frac{1}{2} [(a_m + a_f)(\beta_m - \beta_f) + (a_m - a_f)(\beta_m + \beta_f)], \quad (30)$$

766 which together with **Eq. 29** gives

$$s_m - s_f = \frac{1}{2} \left[(a_m + a_f) + \frac{(a_m - a_f)(a_f - a_m)}{a_f + a_m} \right] (\beta_m - \beta_f) = \frac{2a_m a_f}{a_m + a_f} (\beta_m - \beta_f). \quad (31)$$

767 We denote the heritability due to GxSex at the locus as $V_{GxSex} := 2p(1-p)(\beta_m - \beta_f)^2$ and
768 the parameter relating this contribution to the differentiation in allele frequencies as

$$A := 2 \left(\frac{a_m a_f}{a_m + a_f} \right)^2, \quad (32)$$

769 and plug **Eq. 31** into **Eq. 24**, we get

$$F_{ST} \approx AV_{GxSex}, \quad (33)$$

770 as given by **Eq. 3** in **Results**.

771

772 **Estimating the potential for sexually antagonistic selection on standing variation (A).** For
773 each trait and gnomAD subsample (**Supplementary Materials**), we estimated A using weighted
774 least squares linear regression of our estimate of F_{ST} (\widehat{F}_{ST}) to our estimate of V_{GxSex} (\widehat{V}_{GxSex}), with
775 weight w inversely proportional to our site-specific estimate of noise in the estimate of V_{GxSex} ,

$$w = \frac{1}{\text{Var}[\widehat{V}_{GxSex}]}. \quad (34)$$

776 To simplify the estimation of $\text{Var}[\widehat{V}_{GxSex}]$, we treated the allele frequency p as perfectly
777 estimated, and as independent of the allele frequency in the GWAS sample—as different data
778 are used in the GWAS (UK Biobank) and in the allele frequency estimation (gnomAD). Under
779 these assumptions,

$$\text{Var}[\widehat{V}_{GxSex}] = \text{Var}[2p(1-p)\widehat{D}^2] = [2p(1-p)]^2 \text{Var}[(\hat{\beta}_m - \hat{\beta}_f)^2], \quad (35)$$

780 and thus the task at hand is estimating $\text{Var}[(\hat{\beta}_m - \hat{\beta}_f)^2]$. Using the law of total variance,

$$\text{Var}[(\hat{\beta}_m - \hat{\beta}_f)^2] = \text{Var}_{\hat{\beta}_f} \left[E_{\hat{\beta}_m} [(\hat{\beta}_m - \hat{\beta}_f)^2 | \hat{\beta}_f] \right] + E_{\hat{\beta}_f} \left[\text{Var}_{\hat{\beta}_m} [(\hat{\beta}_m - \hat{\beta}_f)^2 | \hat{\beta}_f] \right]. \quad (36)$$

781 We begin with the argument of the first term,

$$E_{\hat{\beta}_m} [(\hat{\beta}_m - \hat{\beta}_f)^2 | \hat{\beta}_f] = E_{\hat{\beta}_m} [\hat{\beta}_m^2 - 2\hat{\beta}_m \hat{\beta}_f + \hat{\beta}_f^2 | \hat{\beta}_f] = \mu_m^2 + \sigma_m^2 - 2\mu_m \hat{\beta}_f + \hat{\beta}_f^2, \quad (37)$$

782 where we denote

$$\mu_z = E[\hat{\beta}_z]; \quad (38)$$

$$\sigma_z^2 = \text{Var}[\hat{\beta}_z]$$

783 for each sex $z \in \{m, f\}$. Plugging **Eq. 37** into the first term of **Eq. 36**,

$$\begin{aligned} \text{Var}_{\hat{\beta}_f} \left[E_{\hat{\beta}_m} \left[(\hat{\beta}_m - \hat{\beta}_f)^2 \middle| \hat{\beta}_f \right] \right] &= \text{Var}_{\hat{\beta}_f} [\mu_m^2 + \sigma_m^2] + \text{Var}_{\hat{\beta}_f} [\hat{\beta}_f^2 - 2\mu_m \hat{\beta}_f] = \\ 0 + \text{Var}_{\hat{\beta}_f} [\hat{\beta}_f^2 - 2\mu_m \hat{\beta}_f] &= \text{Var}_{\hat{\beta}_f} [\hat{\beta}_f^2] + 4\text{Var}_{\hat{\beta}_f} [\mu_m \hat{\beta}_f] - 4\mu_m \text{Cov}_{\hat{\beta}_f} [\hat{\beta}_f^2, \hat{\beta}_f], \end{aligned} \quad (39)$$

784 where the first and second step follow from the fact that $\mu_m^2 + \sigma_m^2$ is a constant. We can take note
785 of the fact that $\hat{\beta}_z$ is Normally distributed around β_z , and in particular that it has no skewness.
786 Therefore,

$$\text{Cov}_{\hat{\beta}_z} [\hat{\beta}_z^2, \hat{\beta}_z] = E[\hat{\beta}_z^3] - E[\hat{\beta}_z]E[\hat{\beta}_z^2] = (\mu_z^3 + 3\mu_z\sigma_z^2 + \gamma_z\sigma_z^3) - \mu_z(\mu_z^2 + \sigma_z^2) = 2\mu_z\sigma_z^2, \quad (40)$$

787 where $\gamma_z = 0$ is the skewness of $\hat{\beta}_z$. We can also note that

$$\text{Var}_{\hat{\beta}_z} [\hat{\beta}_z^2] = \text{Var}_{\hat{\beta}_z} [(\sigma_z b_z + \mu_z)^2], \quad (41)$$

788 where we defined

$$b_z = \frac{\hat{\beta}_z - \mu_z}{\sigma_z},$$

789 and therefore b_z is a Standard Normal and therefore b_z^2 is Chi-squared with one degree of
790 freedom. **Eq. 41** now gives

$$\begin{aligned} \text{Var}_{\hat{\beta}_z} [\hat{\beta}_z^2] &= \text{Var}_{\hat{\beta}_z} [\sigma_z^2 b_z^2 + 2\sigma_z \mu_z b_z] \\ &= \text{Var}_{\hat{\beta}_z} [\sigma_z^2 b_z^2] + \text{Var}[2\sigma_z \mu_z b_z] + \text{Cov}[\sigma_z^2 b_z^2, 2\sigma_z \mu_z b_z] \\ &= \text{Var}[b_z^2] \sigma_z^4 + 4\text{Var}[b_z] \mu_z^2 \sigma_z^2 + 0 = 2\sigma_z^4 + 4\mu_z^2 \sigma_z^2. \end{aligned} \quad (42)$$

791 Plugging **Eq. 40** and **Eq. 42** into **Eq. 39**, we find

$$\text{Var}_{\hat{\beta}_f} \left[E_{\hat{\beta}_m} \left[(\hat{\beta}_m - \hat{\beta}_f)^2 \middle| \hat{\beta}_f \right] \right] = 2\sigma_f^4 + 4\mu_f^2 \sigma_f^2 + 4\mu_m^2 \sigma_f^2 - 8\mu_m \mu_f \sigma_f^2. \quad (43)$$

792 We now turn to the second term of **Eq. 36**. First,

$$\begin{aligned} \text{Var}_{\hat{\beta}_m} \left[(\hat{\beta}_m - \hat{\beta}_f)^2 \middle| \hat{\beta}_f \right] &= \text{Var}[\hat{\beta}_m^2 + 2\hat{\beta}_m \hat{\beta}_f \middle| \hat{\beta}_f] \\ &= \text{Var}[\hat{\beta}_m^2] + 4\sigma_m^2 \hat{\beta}_f^2 - 4\hat{\beta}_f \text{Cov}[\hat{\beta}_m, \hat{\beta}_m^2]. \end{aligned} \quad (44)$$

793 **Eq. 40** and **42** again give us

$$\text{Var}_{\hat{\beta}_m} \left[(\hat{\beta}_m - \hat{\beta}_f)^2 \middle| \hat{\beta}_f \right] = 2\sigma_m^4 + 4\mu_m^2 \sigma_m^2 + 4\sigma_m^2 \hat{\beta}_f^2 - 8\mu_m \sigma_m^2 \hat{\beta}_f, \quad (45)$$

794 which then gives

$$E_{\hat{\beta}_f} \left[\text{Var}_{\hat{\beta}_m} \left[(\hat{\beta}_m - \hat{\beta}_f)^2 \middle| \hat{\beta}_f \right] \right] = 2\sigma_m^4 + 4\mu_m^2 \sigma_m^2 + 4\sigma_m^2 (\sigma_f^2 + \mu_f^2) - 8\mu_m \mu_f \sigma_m^2. \quad (46)$$

795 Plugging **Eq. 43** and **Eq. 46** into **Eq. 36**, we obtain

$$\text{Var}[(\hat{\beta}_m - \hat{\beta}_f)^2] = \quad (47)$$

$$= 2(\sigma_m^4 + \sigma_f^4) + 4\sigma_m^2\sigma_f^2 + 4(\mu_m^2\sigma_m^2 + \mu_f^2\sigma_f^2) + 4(\sigma_m^2\mu_f^2 + \sigma_f^2\mu_m^2) - 8\mu_m\mu_f(\sigma_m^2 + \sigma_f^2).$$

796 Finally, we estimate μ_z with the GWAS-derived point estimate of the effect $\hat{\beta}_z$ and σ_z with
797 its standard error, $\hat{\sigma}_z = [\hat{\beta}_z]$. Plugging back into **Eq. 35**, we obtain

$$\text{Var}[\widehat{V}_{GxSex}] = [2p(1-p)]^2 [2(\hat{\sigma}_m^4 + \hat{\sigma}_f^4) + 4\hat{\sigma}_m^2\hat{\sigma}_f^2 + 4(\hat{\beta}_m^2\sigma_m^2 + \hat{\beta}_f^2\sigma_f^2) + 4(\hat{\sigma}_m^2\hat{\beta}_f^2 + \hat{\sigma}_f^2\hat{\beta}_m^2) - 8\hat{\beta}_m\hat{\beta}_f(\hat{\sigma}_m^2 + \hat{\sigma}_f^2)]. \quad (48)$$

798 Using **Eq. 33**, we estimate F_{st} with the estimator

$$\widehat{F}_{st} = n_{st}/d_{st}, \quad (49)$$

799 where

$$n_{st} = (\widehat{p}_m - \widehat{p}_f)^2 - SE(\widehat{p}_m)^2 - SE(\widehat{p}_f)^2, \quad (50)$$

$$800 \quad d_{st} = 4\hat{p}(1 - \hat{p}) - SE(\widehat{p}_m)^2 - SE(\widehat{p}_f)^2,$$

801 and noting that

$$E[\widehat{F}_{st}] \approx \frac{E[n_{st}]}{E[d_{st}]} = \frac{(p_m - p_f)^2 - \text{Var}(p_m) + \text{Var}(p_f) + E\{SE(\widehat{p}_m)^2\} + E\{SE(\widehat{p}_f)^2\}}{4p(1-p) + \text{Var}(p_m)^2 + \text{Var}(p_f)^2 - E\{SE(\widehat{p}_m)^2\} - E\{SE(\widehat{p}_f)^2\}} = F_{st}, \quad (51)$$

802 where in the first equality we approximated the expectation of a ratio with the ratio of expectations.
803 Therefore, **Eq. 49** provides an approximately unbiased estimator of F_{st} despite the absence of
804 genotype frequencies.

805 To perform this estimation of A on the GWAS and F_{st} data, we used paired v and V_{GxSex}
806 points for all sites which passed all previous stages of filtering. Weights were set by **Eq. 34** and
807 follow **Eq. 48** where $\hat{\beta}_m$ and $\hat{\beta}_f$ are the GWAS effect estimates as above, and $\hat{\sigma}_m$ and $\hat{\sigma}_f$ are the
808 GWAS standard errors (SE) estimates for the effect size of each site per trait.

809 To minimize the possibility of LD between sites used in the analysis as much as possible,
810 we used the approximately independent LD blocks in Europeans⁷⁶ as in Section “Mixture weights
811 for covariance structure between male and female effects”. Namely, we subdivided the genome
812 into 1703 approximately independent LD blocks as before. We iterated over the 1703 blocks and
813 sampling one site per block in a given iteration, using a sample of (up to) 1703 post-filtering sites
814 to perform the weighted linear regression of F_{ST} on $V_{G \times Sex}$. The slope of this regression was used

815 as an estimate of A . We perform this estimation procedure 1,000 times and take an average of
816 Z scores (slope point estimates divided by their SE) as the final estimate of A . In each replicate,
817 we sample with replacement m LD blocks from the m LD blocks which had at least one site within
818 them post-filtering (Supplementary Materials); we then sample one site per resampled block. In
819 **Fig. 7D**, each point is the mean of the 1,000 samples of one site per LD block and 90% confidence
820 intervals show the range between the 5th and 95th percentile of the 1000 replicates.

821 In the main text, we focus on the results performed this estimation for Ashkenazi Jewish,
822 Finnish, and Non-Finnish European populations as the other ancestry group-stratified
823 subsamples in *gnomAD* are further diverged from the UKB White British sample and therefore
824 our GWAS estimates are expected to be less portable^{57,81}. We also performed a similar analysis
825 using UKB data to measure differentiation in allele frequencies between males and females,
826 rather than an independent dataset (*gnomAD*) as in the main text. Since individual level data was
827 available in this case, we replaced F_{st} with L_{ST} , a measure developed by Ruzicka et al.⁵¹. L_{st} can
828 be thought of as site-specific F_{st} controlled for major axes of population structure differentiating
829 males and females (**Fig. S21**).

830 **References**

- 831 1. van Doorn, G. S. Intralocus sexual conflict. *Ann N Y Acad Sci* **1168**, 52–71 (2009).
- 832 2. Arnqvist, G. & Rowe, L. *Sexual Conflict*. (Princeton University Press, 2005).
833 doi:10.1515/9781400850600.
- 834 3. Barson, N. J. *et al.* Sex-dependent dominance at a single locus maintains variation in age
835 at maturity in salmon. *Nature* **528**, 405–408 (2015).
- 836 4. Kidwell, J. F., Clegg, M. T., Stewart, F. M. & Prout, T. Regions of stable equilibria for models
837 of differential selection in the two sexes under random mating. *Genetics* **85**, 171–83 (1977).
- 838 5. Connallon, T., Cox, R. M. & Calsbeek, R. Fitness consequences of sex-specific selection.
839 *Evolution* **64**, 1671–82 (2010).
- 840 6. Harrison, P. W. *et al.* Sexual selection drives evolution and rapid turnover of male gene
841 expression. *Proceedings of the National Academy of Sciences* **112**, 4393–4398 (2015).
- 842 7. Cheng, C. & Kirkpatrick, M. Sex-Specific Selection and Sex-Biased Gene Expression in
843 Humans and Flies. *PLoS Genet* **12**, e1006170 (2016).
- 844 8. Karp, N. A. *et al.* Prevalence of sexual dimorphism in mammalian phenotypic traits. *Nat*
845 *Commun* **8**, 15475 (2017).
- 846 9. Schroderus, E. *et al.* Intra- and Intersexual Trade-Offs between Testosterone and Immune
847 System: Implications for Sexual and Sexually Antagonistic Selection. *Am Nat* **176**, E90–
848 E97 (2010).

- 849 10. Power, R. A. *et al.* Fecundity of Patients With Schizophrenia, Autism, Bipolar Disorder,
850 Depression, Anorexia Nervosa, or Substance Abuse vs Their Unaffected Siblings. *JAMA*
851 *Psychiatry* **70**, 22 (2013).
- 852 11. Mokkonen, M. & Crespi, B. J. Genomic conflicts and sexual antagonism in human health:
853 insights from oxytocin and testosterone. *Evol Appl* **8**, 307–325 (2015).
- 854 12. Harper, J. A., Janicke, T. & Morrow, E. H. Systematic review reveals multiple sexually
855 antagonistic polymorphisms affecting human disease and complex traits. *Evolution (N Y)*
856 **75**, 3087–3097 (2021).
- 857 13. Oliva, M. *et al.* The impact of sex on gene expression across human tissues. *Science*
858 (1979) **369**, eaba3066 (2020).
- 859 14. Khramtsova, E. A., Davis, L. K. & Stranger, B. E. The role of sex in the genomics of human
860 complex traits. *Nat Rev Genet* **20**, 173–190 (2019).
- 861 15. Clayton, J. A. & Collins, F. S. Policy: NIH to balance sex in cell and animal studies. *Nature*
862 **509**, 282–283 (2014).
- 863 16. Clayton, J. A. Studying both sexes: a guiding principle for biomedicine. *The FASEB Journal*
864 **30**, 519–524 (2016).
- 865 17. Nature journals raise the bar on sex and gender reporting in research. *Nature* **605**, 396–
866 396 (2022).
- 867 18. Sinnott-Armstrong, N., Naqvi, S., Rivas, M. & Pritchard, J. K. Gwas of three molecular traits
868 highlights core genes and pathways alongside a highly polygenic background. *Elife* **10**, 1–
869 35 (2021).

- 870 19. Carole Hooven. *T: The Story of Testosterone, the Hormone that Dominates and Divides*
871 *Us*. (Henry Holt and Co., 2021).
- 872 20. Flynn, E. *et al.* Sex-specific genetic effects across biomarkers. *Eur J Hum Genet* **29**, 154–
873 163 (2021).
- 874 21. Bernabeu, E. *et al.* Sex differences in genetic architecture in the UK Biobank. *Nat Genet*
875 **53**, 1283–1289 (2021).
- 876 22. Muir, W., Nyquist, W. E. & Xu, S. Alternative partitioning of the genotype-by-environment
877 interaction. *Theoretical and Applied Genetics* **84**, 193–200 (1992).
- 878 23. Robertson, A. The Sampling Variance of the Genetic Correlation Coefficient. *Biometrics*
879 **15**, 469 (1959).
- 880 24. Falconer, D. S. The Problem of Environment and Selection. *Am Nat* **86**, 293–298 (1952).
- 881 25. Fry, J. D. The Mixed-Model Analysis of Variance Applied to Quantitative Genetics:
882 Biological Meaning of the Parameters. *Evolution (N Y)* **46**, 540 (1992).
- 883 26. Yamada, Y. Genotype by Environment Interaction and Genetic Correlation of the same
884 Trait under Different Environments. *The Japanese Journal of Genetics* **37**, 498–509 (1962).
- 885 27. Brown, B. C., Asian Genetic Epidemiology Network Type 2 Diabetes Consortium, Ye, C.
886 J., Price, A. L. & Zaitlen, N. Transethnic Genetic-Correlation Estimates from Summary
887 Statistics. *Am J Hum Genet* **99**, 76–88 (2016).
- 888 28. Galinsky, K. J. *et al.* Estimating cross-population genetic correlations of causal effect sizes.
889 *Genet Epidemiol* **43**, 180–188 (2019).

- 890 29. Ni, G., Moser, G., Schizophrenia Working Group of the Psychiatric Genomics Consortium,
891 Wray, N. R. & Lee, S. H. Estimation of Genetic Correlation via Linkage Disequilibrium Score
892 Regression and Genomic Restricted Maximum Likelihood. *Am J Hum Genet* **102**, 1185–
893 1194 (2018).
- 894 30. Shi, H., Mancuso, N., Spendlove, S. & Pasaniuc, B. Local Genetic Correlation Gives
895 Insights into the Shared Genetic Architecture of Complex Traits. *The American Journal of*
896 *Human Genetics* **101**, 737–751 (2017).
- 897 31. Bulik-Sullivan, B. K. *et al.* An atlas of genetic correlations across human diseases and traits.
898 *Nat Genet* **47**, 1236–1241 (2015).
- 899 32. DiMarco, M., Zhao, H., Boulicault, M. & Richardson, S. S. Why “sex as a biological variable”
900 conflicts with precision medicine initiatives. *Cell Rep Med* **3**, 100550 (2022).
- 901 33. Lumish, H. S., O’Reilly, M. & Reilly, M. P. Sex Differences in Genomic Drivers of Adipose
902 Distribution and Related Cardiometabolic Disorders: Opportunities for Precision Medicine.
903 *Arteriosclerosis, thrombosis, and vascular biology* vol. 40 45–60 Preprint at
904 <https://doi.org/10.1161/ATVBAHA.119.313154> (2020).
- 905 34. Boyle, E. A., Li, Y. I. & Pritchard, J. K. An Expanded View of Complex Traits: From
906 Polygenic to Omnigenic. *Cell* **169**, 1177–1186 (2017).
- 907 35. Shi, H., Kichaev, G. & Pasaniuc, B. Contrasting the Genetic Architecture of 30 Complex
908 Traits from Summary Association Data. *Am J Hum Genet* **99**, 139–53 (2016).
- 909 36. Sella, G. & Barton, N. H. Thinking About the Evolution of Complex Traits in the Era of
910 Genome-Wide Association Studies. *Annu Rev Genomics Hum Genet* **20**, 461–493 (2019).

- 911 37. Bulik-Sullivan, B. K. *et al.* LD Score regression distinguishes confounding from polygenicity
912 in genome-wide association studies. *Nat Genet* **47**, 291–295 (2015).
- 913 38. Benonisdottir, S. & Kong, A. The Genetics of Participation: Method and Analysis. *bioRxiv*
914 (2022) doi:10.1101/2022.02.11.480067.
- 915 39. Lynch, M. & Walsh, B. *Genetics and Analysis of Quantitative Traits*. (Sinauer Associates,
916 1998).
- 917 40. Urbut, S. M., Wang, G., Carbonetto, P. & Stephens, M. Flexible statistical methods for
918 estimating and testing effects in genomic studies with multiple conditions. *Nat Genet* **51**,
919 187–195 (2019).
- 920 41. Pasquali, R. Obesity and androgens: facts and perspectives. *Fertil Steril* **85**, 1319–40
921 (2006).
- 922 42. Domingue, B. W., Kanopka, K., Mallard, T. T., Trejo, S. & Tucker-Drob, E. M. Modeling
923 Interaction and Dispersion Effects in the Analysis of Gene-by-Environment Interaction.
924 *Behav Genet* **52**, 56–64 (2022).
- 925 43. Liu, D. *et al.* Skeletal muscle gene expression in response to resistance exercise: sex
926 specific regulation. *BMC Genomics* **11**, 659 (2010).
- 927 44. Lutz, S. Z. *et al.* Sex-Specific Associations of Testosterone With Metabolic Traits. *Front*
928 *Endocrinol (Lausanne)* **10**, (2019).
- 929 45. Kraemer, W. J., Ratamess, N. A. & Nindl, B. C. Recovery responses of testosterone,
930 growth hormone, and IGF-1 after resistance exercise. *J Appl Physiol* **122**, 549–558 (2017).

- 931 46. Roberts, B. M., Nuckols, G. & Krieger, J. W. Sex Differences in Resistance Training: A
932 Systematic Review and Meta-Analysis. *J Strength Cond Res* **34**, 1448–1460 (2020).
- 933 47. Zajitschek, S. R. *et al.* Sexual dimorphism in trait variability and its eco-evolutionary and
934 statistical implications. *Elife* **9**, (2020).
- 935 48. Kasimatis, K. R. *et al.* Evaluating human autosomal loci for sexually antagonistic viability
936 selection in two large biobanks. *Genetics* **217**, (2021).
- 937 49. Ryan, M. *The Genetics of Political Behavior*. (Routledge, 2020).
- 938 50. Ruzicka, F., Holman, L. & Connallon, T. Polygenic signals of sexually antagonistic selection
939 in contemporary human genomes. *bioRxiv* (2021) doi:10.1101/2021.09.20.461171.
- 940 51. Ruzicka, F. *et al.* The search for sexually antagonistic genes: Practical insights from studies
941 of local adaptation and statistical genomics. *Evol Lett* **4**, 398–415 (2020).
- 942 52. Wright, S. The genetical structure of populations. *Ann Eugen* **15**, 323–54 (1951).
- 943 53. Weir, B. S. & Cockerham, C. C. Estimating F-Statistics for the Analysis of Population
944 Structure. *Evolution (N Y)* **38**, 1358 (1984).
- 945 54. Karczewski, K. J. *et al.* The mutational constraint spectrum quantified from variation in
946 141,456 humans. *Nature* **581**, 434–443 (2020).
- 947 55. Pirastu, N. *et al.* Genetic analyses identify widespread sex-differential participation bias.
948 *Nat Genet* **53**, 663–671 (2021).

- 949 56. Bissegger, M., Laurentino, T. G., Roesti, M. & Berner, D. Widespread intersex
950 differentiation across the stickleback genome – The signature of sexually antagonistic
951 selection? *Mol Ecol* **29**, 262–271 (2020).
- 952 57. Privé, F. *et al.* Portability of 245 polygenic scores when derived from the UK Biobank and
953 applied to 9 ancestry groups from the same cohort. *The American Journal of Human*
954 *Genetics* **109**, 12–23 (2022).
- 955 58. Traglia, M., Bout, M. & Weiss, L. A. Sex-heterogeneous SNPs disproportionately influence
956 gene expression and health. *PLoS Genet* **18**, e1010147 (2022).
- 957 59. Berg, J. J. *et al.* Reduced signal for polygenic adaptation of height in UK Biobank. *Elife* **8**,
958 (2019).
- 959 60. Sohail, M. *et al.* Polygenic adaptation on height is overestimated due to uncorrected
960 stratification in genome-wide association studies. *Elife* **8**, (2019).
- 961 61. Young, A. I., Benonisdottir, S., Przeworski, M. & Kong, A. Deconstructing the sources of
962 genotype-phenotype associations in humans. *Science* **365**, 1396–1400 (2019).
- 963 62. Coop, G. & Przeworski, M. Lottery, luck, or legacy. A review of “The Genetic Lottery: Why
964 DNA matters for social equality”. *Evolution (N Y)* **76**, 846–853 (2022).
- 965 63. Mills, M. C. & Tropf, F. C. Sociology, Genetics, and the Coming of Age of Sociogenomics.
966 *Annu Rev Sociol* **46**, 553–581 (2020).
- 967 64. Coop, G. Reading tea leaves? Polygenic scores and differences in traits among groups.
968 Preprint at (2019).

- 969 65. Ober, C., Loisel, D. A. & Gilad, Y. Sex-specific genetic architecture of human disease. *Nat*
970 *Rev Genet* **9**, 911–922 (2008).
- 971 66. Khan, S. S. *et al.* Association of Body Mass Index With Lifetime Risk of Cardiovascular
972 Disease and Compression of Morbidity. *JAMA Cardiol* **3**, 280 (2018).
- 973 67. Vazquez, G., Duval, S., Jacobs, D. R. & Silventoinen, K. Comparison of Body Mass Index,
974 Waist Circumference, and Waist/Hip Ratio in Predicting Incident Diabetes: A Meta-
975 Analysis. *Epidemiol Rev* **29**, 115–128 (2007).
- 976 68. Ning, Y., Wang, L. & Giovannucci, E. L. A quantitative analysis of body mass index and
977 colorectal cancer: findings from 56 observational studies. *Obesity Reviews* **11**, 19–30
978 (2010).
- 979 69. Brown, C. D. *et al.* Body Mass Index and the Prevalence of Hypertension and Dyslipidemia.
980 *Obes Res* **8**, 605–619 (2000).
- 981 70. Arthur, R. S., Dannenberg, A. J. & Rohan, T. E. The association of prediagnostic circulating
982 levels of cardiometabolic markers, testosterone and sex hormone-binding globulin with risk
983 of breast cancer among normal weight postmenopausal women in the UK Biobank. *Int J*
984 *Cancer* **149**, 42–57 (2021).
- 985 71. Wang, J. *et al.* Sex-specific associations of circulating testosterone levels with all-cause
986 and cause-specific mortality. *Eur J Endocrinol* **184**, 723–732 (2021).
- 987 72. Fry, A. *et al.* Comparison of Sociodemographic and Health-Related Characteristics of UK
988 Biobank Participants With Those of the General Population. *Am J Epidemiol* **186**, 1026–
989 1034 (2017).

- 990 73. Bycroft, C. *et al.* The UK Biobank resource with deep phenotyping and genomic data.
991 *Nature* **562**, 203–209 (2018).
- 992 74. Haworth, S. *et al.* Apparent latent structure within the UK Biobank sample has implications
993 for epidemiological analysis. *Nat Commun* **10**, 333 (2019).
- 994 75. Stephens, M. False discovery rates: a new deal. *Biostatistics* kxw041 (2016)
995 doi:10.1093/biostatistics/kxw041.
- 996 76. Berisa, T. & Pickrell, J. K. Approximately independent linkage disequilibrium blocks in
997 human populations. *Bioinformatics* **32**, 283–5 (2016).
- 998 77. Sudlow, C. *et al.* UK Biobank: An Open Access Resource for Identifying the Causes of a
999 Wide Range of Complex Diseases of Middle and Old Age. *PLoS Med* **12**, e1001779 (2015).
- 1000 78. Davies, N. M., Holmes, M. v & Davey Smith, G. Reading Mendelian randomisation studies:
1001 a guide, glossary, and checklist for clinicians. *BMJ* k601 (2018) doi:10.1136/bmj.k601.
- 1002 79. Davey Smith, G. & Ebrahim, S. ‘Mendelian randomization’: can genetic epidemiology
1003 contribute to understanding environmental determinants of disease?*. *Int J Epidemiol* **32**,
1004 1–22 (2003).
- 1005 80. Gillespie, J. H. *Population Genetics: A Concise Guide*. (Johns Hopkins University Press,
1006 2004).
- 1007 81. Wang, Y. *et al.* Theoretical and empirical quantification of the accuracy of polygenic scores
1008 in ancestry divergent populations. *Nat Commun* **11**, 3865 (2020).
- 1009